Natural Resources Canada | Ressources naturelles Canada

CANMET Mining and Mineral Sciences Laboratories
Laboratoires des mines et des sciences minérales de CANMET

DIVISION REPORT / RAPPORT DIVISION

Metal Background and Mobility at Christal Lake, Keno Hill Mining District, Yukon

Y.T.J. Kwong[1], S. Arrell[2], E. Soprovich[2], P. Roach[3], M. Guilbeault[2], and J. Miller[2]

[1] CanmetMINING, Ottawa, Natural Resources Canada
[2] Environmental Protection Services, Environment Canada, Whitehorse
[3] Aboriginal Affairs and Northern Development Canada, Whitehorse

Project: **MMSL No. 603556**
Project Title: Metal Background and Mobility at the Keno Hill

DIVISION REPORT MMSL 11-008 (TR) **Final Version: October 2013**

EXECUTIVE SUMMARY

Historic mines in the Keno Hill mining district, Yukon Territory, are currently under reclamation while new mining and exploration activities flourish in the area. To aid with setting practical sediment quality guidelines for various on-going and potential projects CanmetMINING and technical staff from Aboriginal Affairs and Northern Development Canada and Environment Canada designed a collaborative study to determine the metal background and mobility in the historic mining district. Christal Lake, a small lake located at the centre of the district and a short stretch of the creek downstream, both receivers of erosion products and drainage from the surrounding mines, were carefully sampled for a variety of detailed studies. Geochemical analyses coupled with ^{210}Pb age dating of a finely sliced (5 -10 mm) sediment core from the lake show good correlation of sediment metal contents with past and recent mining and reclamation activities. Lake and creek sediments, and by implication soils in mineralized terrains in the Keno Hill area, are generally enriched in As, Cd, and Zn and, to a lesser extent, Cu, Ni, and Pb. Mining-related activities have increased the average Cd and Zn contents in near-surface sediments by 1.6 and 10 times relative to their background values while the As and Pb concentrations do not change significantly. Integration of the sediment geochemistry with water monitoring data at the lake and downstream drainage indicates that, despite the near-neutral to slightly basic pH in the drainage system, Zn and Cd are readily mobilized while As, Cu, Ni and Pb are not. Redox cycling of Mn and secondary carbonate precipitation under freezing conditions appear to control the downstream migration of dissolved Zn and some Cd. These processes render Christal Lake a net sink for dissolved Zn. In conclusion, the elevated background metal/metalloid levels in sediments/soil justify site/drainage-specific sediment guidelines for reclamation and mining operations in the district. The roles of microbes and metal-organic matter interaction in attenuating aqueous contaminant transport in this drainage system need to be further investigated to determine if natural attenuation can be relied upon to assist with remediating drainage from the many historic mines in the district.

TABLE OF CONTENTS

FIGURES

TABLES

APPENDICES

INTRODUCTION

Project Background

The Keno Hill mining district in the Yukon Territory was once Canada's second largest silver producer after Ontario's historic Cobalt mining camp. More than 65 vein silver ore deposits and prospects occur in a belt about 8 km wide and 22 km long around Galena Hill and Keno Hill (Figure 1). Silver, lead and zinc deposits were first discovered on Galena Hill in 1906. Mining in the district occurred intermittently between 1919 and 1989. From 1919 to 1939, mining operations primarily entailed manual extraction of high-grade ores on a small scale, which were shipped to the United States of America for processing. In 1946 United Keno Hill Mines Limited (UKHM) started large-scale mining and milling operations in Elsa, which lasted until 1989. While the reclamation of several old sites is in progress, the start-up of a new operation exploiting remnant and newly found mineralization associated with the Bellekeno deposit located near Keno City in 2010, and plans for reopening additional mines in the area signify renewed mining interest in the district. Given the historic environmental legacies, it is a challenge to set practical sediment and water quality guidelines for permitting new mines and reclaiming old sites. In collaboration with technical staff from Environment Canada and Aboriginal Affairs and Northern Development Canada in Whitehorse, CanmetMINING initiated a research project in July 2008 to study the metal background and mobility at Christal Lake near Keno City to help address the issue. This report documents the objectives and scope of the work, the results obtained and conclusions reached in the investigation.

Objectives

The primary objectives of the project are twofold:

1. To establish the background sediment metal levels in a mineralized area in the mining district to facilitate setting appropriate criteria for decommissioning old mines and permitting new ones; and,

2. To identify the major metal remobilization and attenuation processes occurring in the Christal Lake/Christal Creek drainage system so as to inform developing proper strategies for mine waste management and effluent treatment in new mining as well as decommissioning projects in the Keno Hill mining district.

Approach and Scope

The study focuses on detailed sampling and analysis of sediments from Christal Lake, a small lake located near the centre of the mining district (Figure 1) that receives sediment and drainage from several historic operations, some of which are currently undergoing reclamation. As silver mineralization is generally similar across the mining district (Boyle, 1965), the background metal levels in the region could be determined by coupling age-dating with geochemical analysis of a carefully sectioned sediment core from Christal Lake. Additional geochemical and mineralogical characterization of complementary sediment cores from the lake and downstream along Christal Creek in conjunction with water chemistry would shed light on the processes of aqueous metal transport and attenuation in the drainage system. Where appropriate, archived surface water monitoring data are used to probe seasonal effects. The findings are then compared with previous observations documented in the literature and recent observations at other sites to assess their validity across the district. It should be noted that due to budgetary constraints, the investigation is by no means comprehensive. Based on the preliminary findings, recommendations for further work to advance the knowledge of aqueous metal transport and attenuation in the Keno Hill mining district are made at the end of the report.

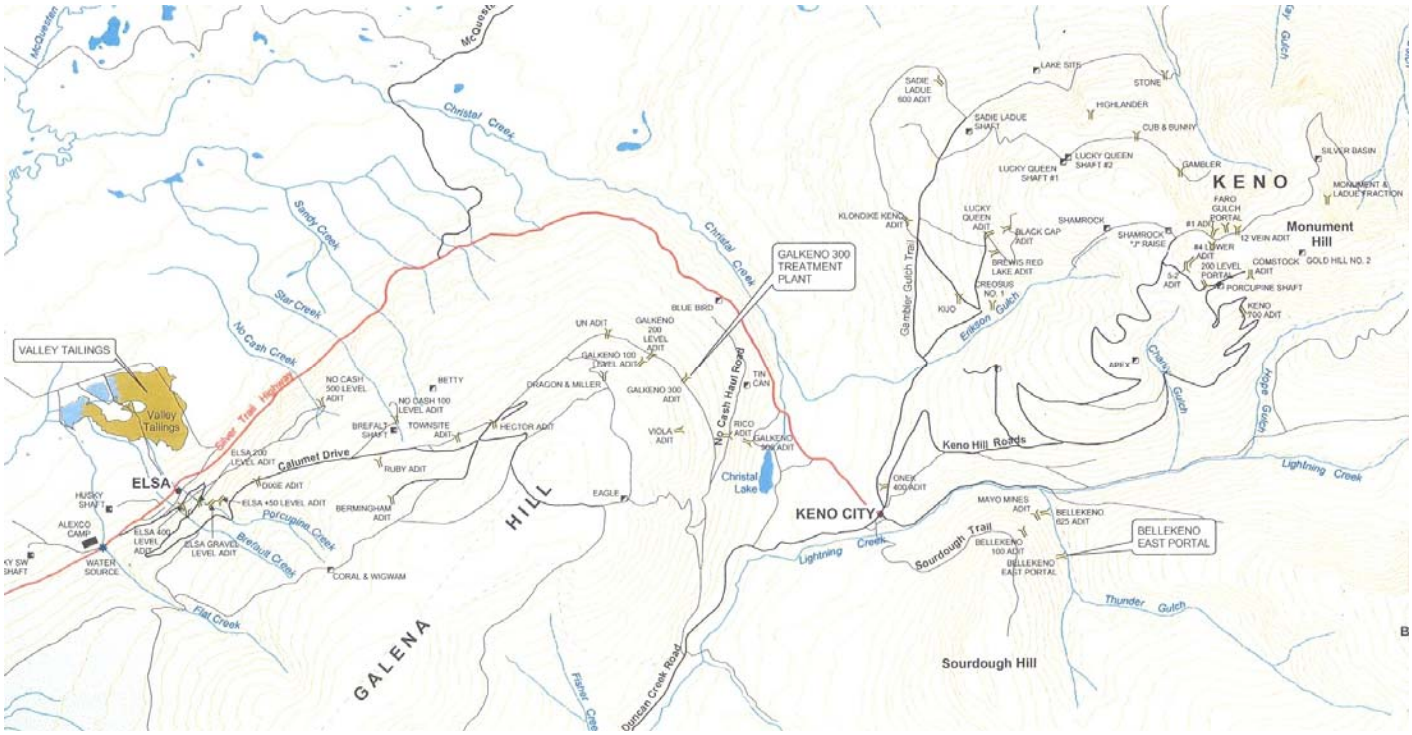

Figure 1: Distribution of silver mineralization in the Keno Hill mining district and the location of Christal Lake.

METHODS

Field Sampling

Sediment coring in Christal Lake was conducted from a boat using a 5.1 cm inner-diameter, 1-m long and transparent plexiglass tube attached to the metal head of a gravity corer to facilitate efficient sediment penetration and core retrieval by hand. Eight locations were sampled on August 27, 2008 (marked as CL-1, CL-2, CL-A, CL-B, CL-C, CL-D, CL-G and CL-H in Figure 2), including duplicate cores from Sites CL-B, CL-C and CL-G. The sampling sites closely matched those of previous water sampling programs in Christal Lake and new sites were chosen based upon field observations at the time of sampling. Prior to sediment sampling, the water depth, temperature, pH, specific conductance, oxidation-reduction potential (ORP) and dissolved oxygen in the overlying water were measured using a HydroLab^{TM} multi-parameter water quality monitor. At sites CL-A and CL-B where the water depth exceeded 1 m (at 1.1 and 2.5 m,

respectively), the same parameters were measured at various depths to ascertain the absence of a thermocline at the time of sampling.

Once ashore the lake sediments, except for two duplicate cores from Sites CL-B and CL-C, (which were reserved for archiving purpose and age dating, respectively), were extracted from the plexiglass tube, sectioned and placed into individual plastic bags according to notable differences in texture and colour. The sectioned samples and the two reserved intact cores were stored in a cooler packed with ice for transport back to Whitehorse and subsequently shipped to various laboratories for different analyses.

In addition, sediment cores were sampled on August 27 and 28, 2011 from five sites downstream of Christal Lake (CCR-1, 2, 3 and 4, and DS KENO RD in Figure 2) using a 5.1 cm inner diameter plexiglass tube. The same field parameters were measured at each of these stream sites as in Christal Lake and the collected samples were subdivided the same way as the lake sediments.

Prior to sediment collection at each sampling site, water samples were collected at mid-depth for a comprehensive suite of analyses including dissolved and total metals, major anions, total dissolved solids as well as acidity and alkalinity. Samples for dissolved metals analysis were filtered at the time of collection through 0.45 μm cellulose nitrate filters and preserved with ultra-pure nitric acid in the field. The other samples, except those for total metals analysis, were also filtered but not acidified. All the water samples were packed in a cooler with ice and subsequently shipped to Environment Canada's analytical laboratory, the Pacific Environment Science Centre, in North Vancouver for analysis.

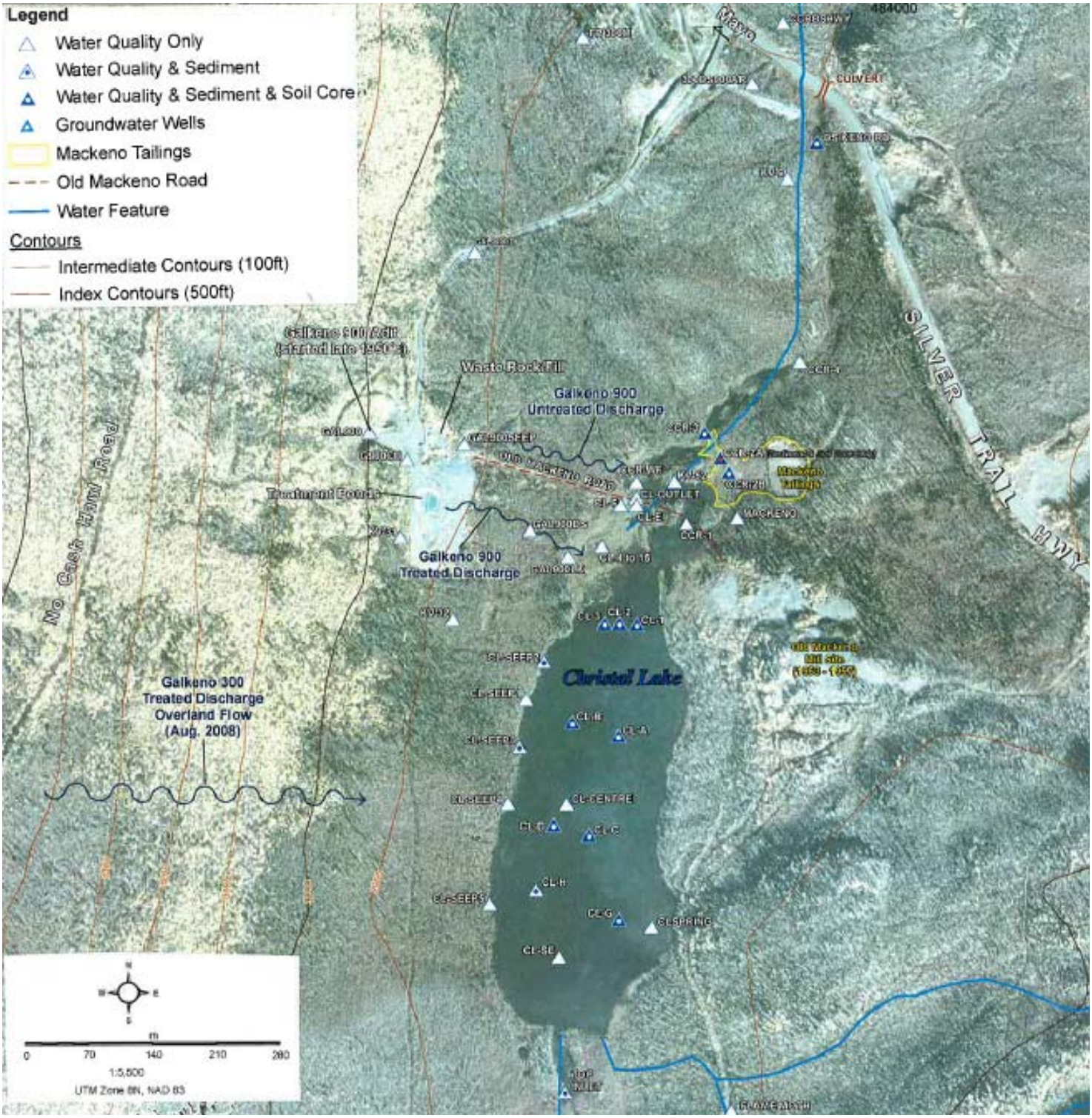

Figure 2: Sampling locations in and around Christal Lake

Laboratory Analyses

The sediment core (CL-C: 27 cm long) reserved for age dating was shipped frozen to the Fresh Water Institute, Winnipeg, where it was sectioned at 0.5 cm increments for the first 10 cm and at 1 cm increments for the remainder of the core. After freeze-drying, a subsample of each slice was sent to Acme Analytical Laboratory Ltd., Vancouver, for whole rock analysis (which includes major oxides and trace elements) using established methods. The radionuclide ^{210}Pb in another subsample of each slice was measured according to the procedure documented by Wilkinson and Simpson (2003). The resulting data were used to determine sedimentation rates and assign dates to the core segments. Specifically, the ages of the sediment slices were estimated using the constant rate of supply (CRS) model of Appelby and Oldfield (1978) which, as shown later, appears to give satisfactory results compatible with field observations.

With the exception of the duplicate cores CL-B (for archiving) and CL-C (for age-dating), all the lake and stream sediments were shipped frozen to CanmetMINING, Ottawa, for mineralogical analysis and limited leach testing. Shortly before the analyses, these samples were thawed and subsamples taken and freeze-dried for X-Ray diffraction (XRD) analysis and examination by scanning electron microscopy (SEM). For XRD analysis, the freeze-dried subsamples were pulverized to a grain size of about 3 μm. Sample pulverization was not required for the SEM work. In addition, the concentration of selected heavy metals in these samples, including Co, Fe, Mn, Ni, Pb, Ti and Zn, were measured semi-quantitatively using a hand-held, field X-Ray fluorescence (XRF) spectrometer.

Due to time and budgetary constraints, powder X-Ray diffractometry (XRD) was the main method utilized to determine the mineralogy of the sediment samples, including subsamples of the duplicate core CL-C remaining from the whole rock and ^{210}Pb analyses. Powder XRD patterns were acquired using a Rigaku D/MAX 2500 rotating anode powder diffractometer with monochromatic CuKα radiation operated under the conditions of 50 kV and 260 mA, a scan speed of 1^{o}/min, step size of 0.02^{o} and a 2θ angular range of $5\text{-}70^{o}$. Phase identification was achieved using the JADE Version 9 software coupled with the ICSD and ICDD databases. Selected samples in the form of loose-grain mounts were examined using a variable-pressure

scanning electron microscope (VP-SEM). A subsample of the material of interest was spread over a carbon tape adhered to an aluminum stub, which was then loaded into the sample chamber of a Hitachi Model S-3200N VP-SEM equipped with an energy-dispersive X-Ray analyser. The sample was examined at different magnifications under the typical operating conditions of 20 kV accelerating voltage, 20 Pa air pressure and a working distance of 15 mm. Through secondary and backscattered electron imaging, X-Ray mapping and spot analysis, the morphology and composition of the overall sample and grains of special interest were recorded.

As the moisture content of most of the collected sediments appeared to be low, there was a concern that insufficient water could be extracted for porewater analysis. Instead, the segmented core samples were subjected to a rapid distilled-water leach using a procedure modified after the USGS Field Leach Test (Hageman, 2005, 2007). A subsample (about 100 g) of each sediment sample was first centrifuged at 10,000 rpm to separate excess porewater. After homogenization, ten grams (wet weight) of the residue were weighed into a 50 mL test tube, and 20 mL of distilled water was added. After capping, the test tube was hand-shaken end-to-end for 2 minutes and then let stand for 20 minutes. The supernatant was filtered through a 0.45 μm filter and preserved with a few drops of ultra-pure nitric acid for the analysis of dissolved constituents by inductively coupled plasma atomic emission spectrometry (ICP-AES). The acquired data would provide insight on the porewater chemistry as well as the presence of readily soluble minerals.

RESULTS AND INTERPRETATION

Geochemistry and Mineralogy of the Dated Core

The temporal change in sedimentation rates at Christal Lake based on ^{210}Pb dating of the core CL-C according to the CRS model is depicted in Figure 3. The higher sedimentation rates observed between the late 1940s to about 1970 and since about 2000 are in general agreement with the intensity of mining and reclamation activities, respectively, occurring in the district. Major events that could have affected sediment loading to the lake are summarized in Table 1.

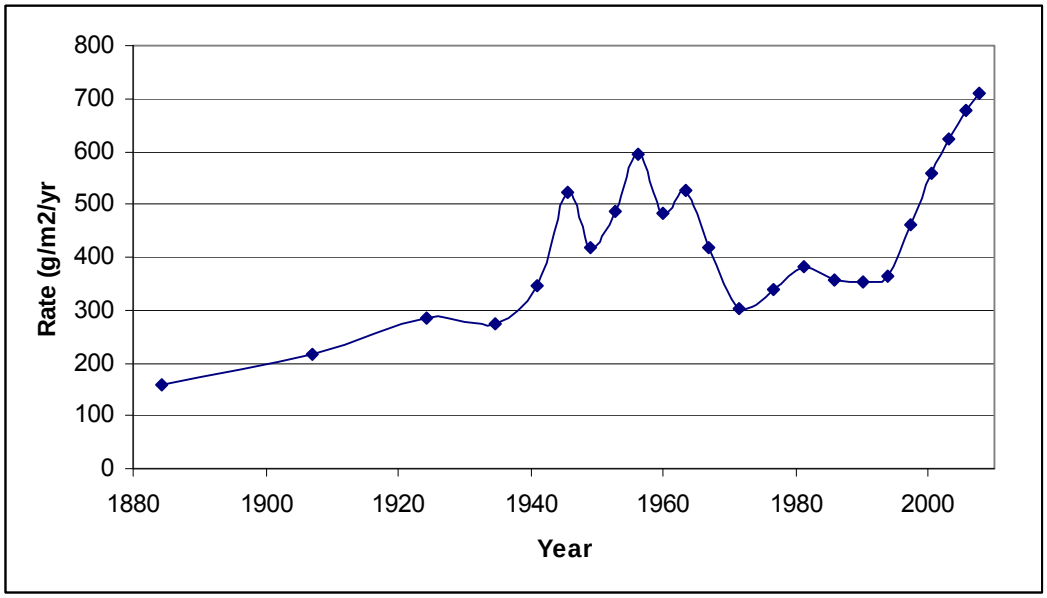

Figure 3: Variation in sedimentation rates in Christal Lake according to the CRS Model.

Table 1: Summary of events affecting sediment loading to Christal Lake

Date	Event
1906	Silver, lead and zinc deposits discovered on Galena Hill
1953-57	Operation of MacKeno mill near the east shore of Christal Lake and tailings deposition near the north end of the lake
Late 1950s	Galkeno 900 Adit started
1959	Extension of Galkeno 900 Adit begun
Late 1960	Breach of underground spring leading to unstoppable discharge flowing out of Galkeno 900 adit, along ~500m of hillside into Christal Lake
1993	Bulkhead installed at Galkeno 900 adit to reduce flow but treated discharge continued to flow to Christal Lake
1998-2006	United Keno Hill mines under care and maintenance
2006	Reclamation activity started
2008-present	Influx of overland flow of treated discharge from Galkeno 300 to Christal Lake

Several elements including As, Cd, Cu, Mn, Ni, Pb and Zn are commonly associated with the silver mineralization in the Keno Hill area (Boyle, 1965). The variation of these elements with depth and time as revealed in analysis of the sectioned core CL-C is shown in Figure 4. Evidently, the top 5 cm of the core is significantly enriched in Mn, Zn, Ni and Cd and slightly impoverished in Cu, Pb and As relative to the bottom of the core (Figure 4, top plot). The relative enrichment of Mn, Zn, Ni and Cd and the relative depletion of Cu, Pb and As in the depositing lake sediments became prominent shortly before 1960 (Figure 4, lower plot) when larger-scale exploration (e.g. development of the Galkeno 900 adit in the late 1950s to 1961), mining and subsequent mine waste and effluent treatment commenced. The observed changes in sediment geochemistry can be explained by the removal of silver-bearing galena (source of Pb) and sulphosalts (source of Cu and As) from the system with progressive mining, leaving behind materials enriched in gangue minerals such as sphalerite (source of Zn, Cd and Ni) and manganese-rich carbonates on the surface. Through erosion processes, some of these gangue materials were transported and subsequently deposited in Christal Lake.

Assuming that the lake sediment chemistry prior to 1940 (when the sedimentation rate started to drastically increase as a result of mining and later some reclamation activities (Figure 3)) truly reflects that of the source materials, then the average metal concentrations of the bottom five slices of the analysed core would represent the background metal levels in the district, prior to intensive mining and related activities. In this case, the background levels of sediment metals/metalloids of concern in the Keno Hill mining district are calculated to be 344 ± 8.7 ppm As, 6.0 ± 0.25 ppm Cd, 52 ± 2.4 ppm Cu, 30 ± 1.1 ppm Ni, 43 ± 1.3 ppm Pb and 796 ± 77 ppm Zn. As shown in Figure 4, mining-related activities increased the average Cd and Zn contents in the near-surface sediments by 1.6 and 10 times, respectively, relative to their background values while the As and Pb concentrations decreased slightly, likely due to ore removal/extraction.

Another notable observation regarding the elemental profiles plotted in Figure 4 is the close resemblance of the Cd and Ni profiles with that of Zn, and the As and Cu profiles with that of Pb. The strong correlation of Cd, Ni and Zn suggests that they are hosted by the same mineral (e.g. sphalerite) and the correlation between As, Cu and Pb implies their co-occurrence in a sulphosalt such as tennatite. Although the Mn and Zn profiles look very similar they are not

identical (which is more obvious in the lower plot of Figure 4), suggesting that the two metals may not be sourced in the same mineral. The linear relationship between Cd and Zn and the relationship between Mn and Zn are depicted in Figure 5. The relationship between Mn and Zn is interesting; there is a strong correlation at low concentrations that is not present at high concentrations of the elements. It should be noted that the high concentrations of both elements occurs in the upper few sediment slices (i.e. at shallow depths). The deviation is biased towards higher Zn concentrations. This suggests that recent effluent treatment may have resulted in the formation of certain Zn-dominated phases with a higher Zn/Mn ratio than the natural alteration products, both of which are eventually transported to and deposited in Christal Lake.

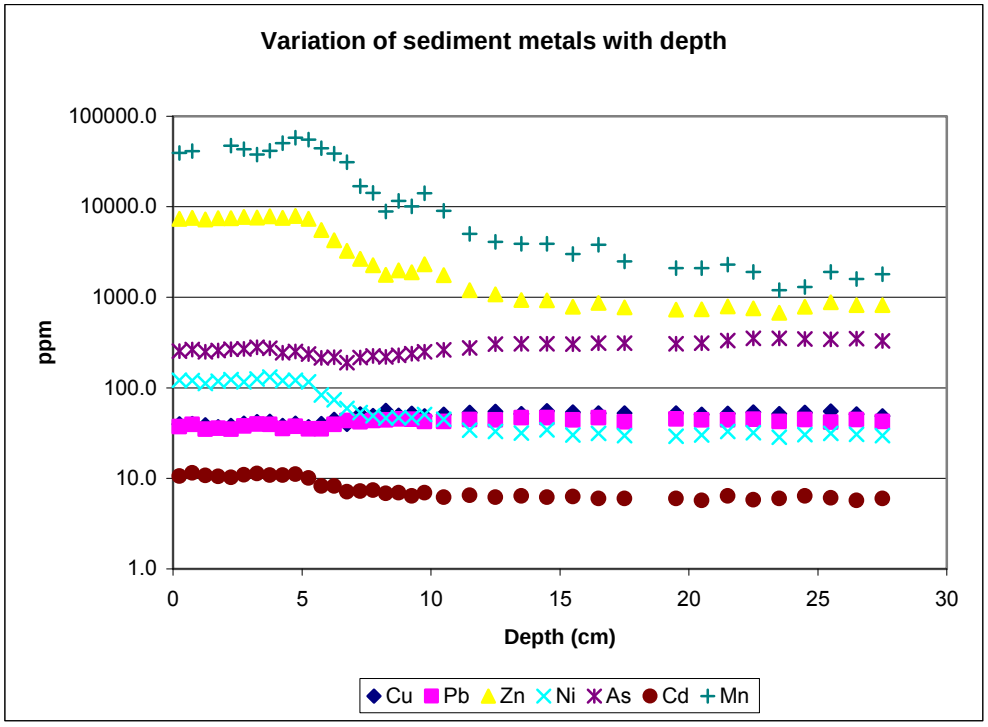

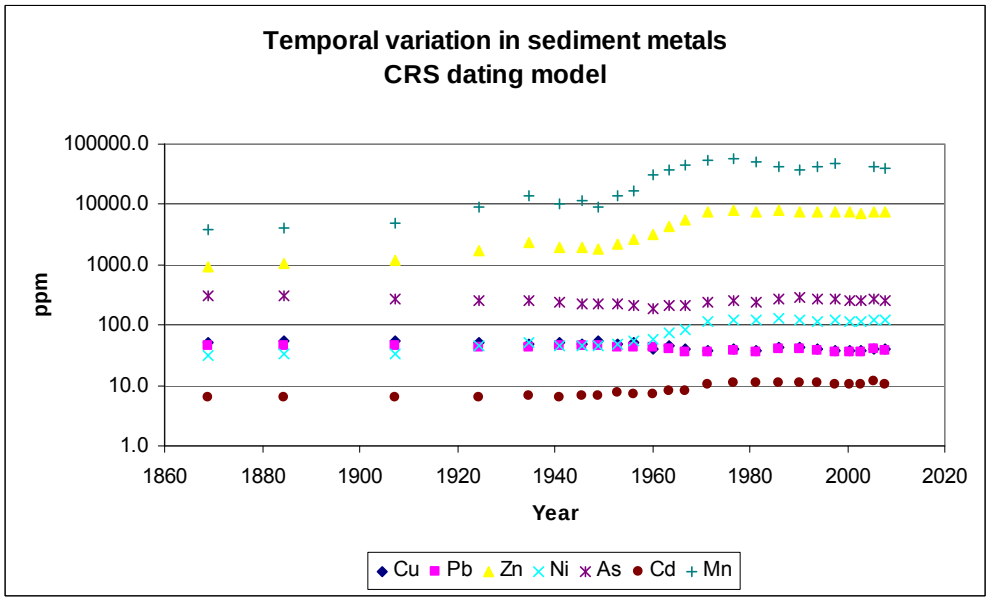

Figure 4: Variation of selected elements in a sediment profile from Christal Lake with depth (upper plot) and time (lower plot) as revealed by ^{210}Pb dating and geochemical analysis.

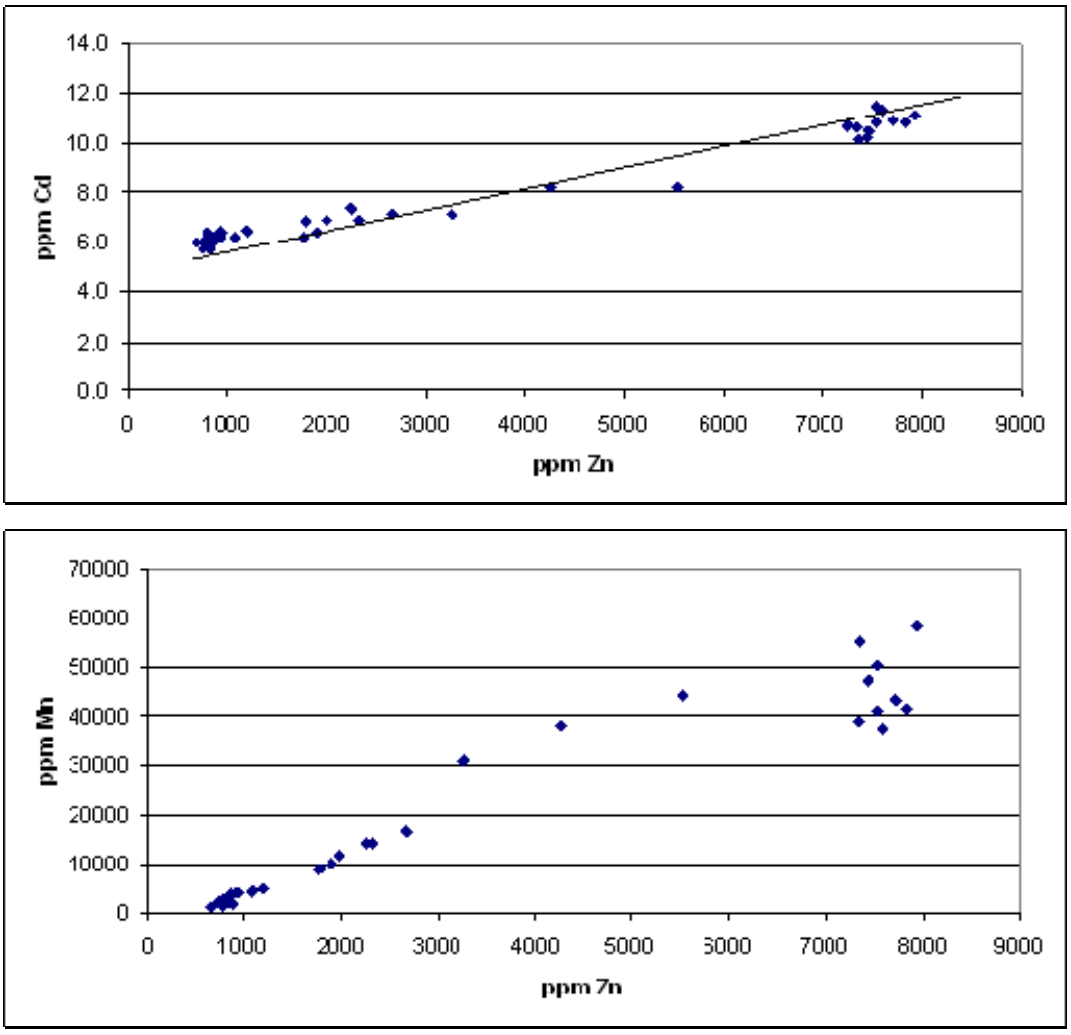

Figure 5: Variation of Cd with Zn (top) and Mn with Zn (bottom) in the sediment core CL-C from Christal Lake

In addition to the trace elements, several major oxides in the sliced sediment core show significant variation with depth, and by extension, time (Figure 6). The drastic increase in CaO content since about 1960 is likely due to the use of lime in effluent treatment, resulting in the formation of secondary calcium sulphate and carbonate phases. The introduction of these secondary phases to the lake diluted the relative contribution of quartz and aluminium silicates to the bulk sediment chemistry and hence the concomitant decrease in SiO_2 and Al_2O_3 contents (Figure 6). Because of the relatively smaller concentrations of MgO, Na_2O and TiO_2 in the sediments, the dilution effect is less obvious for these oxides. The Fe_2O_3 content has not changed much, probably due to continual introduction of hydrated iron oxides to the system,

either as detrital materials or in-situ precipitates. Overall, the observed changes in major element contents with time suggest dominant physical sedimentation prior to 1960 and increased chemical sedimentation since then.

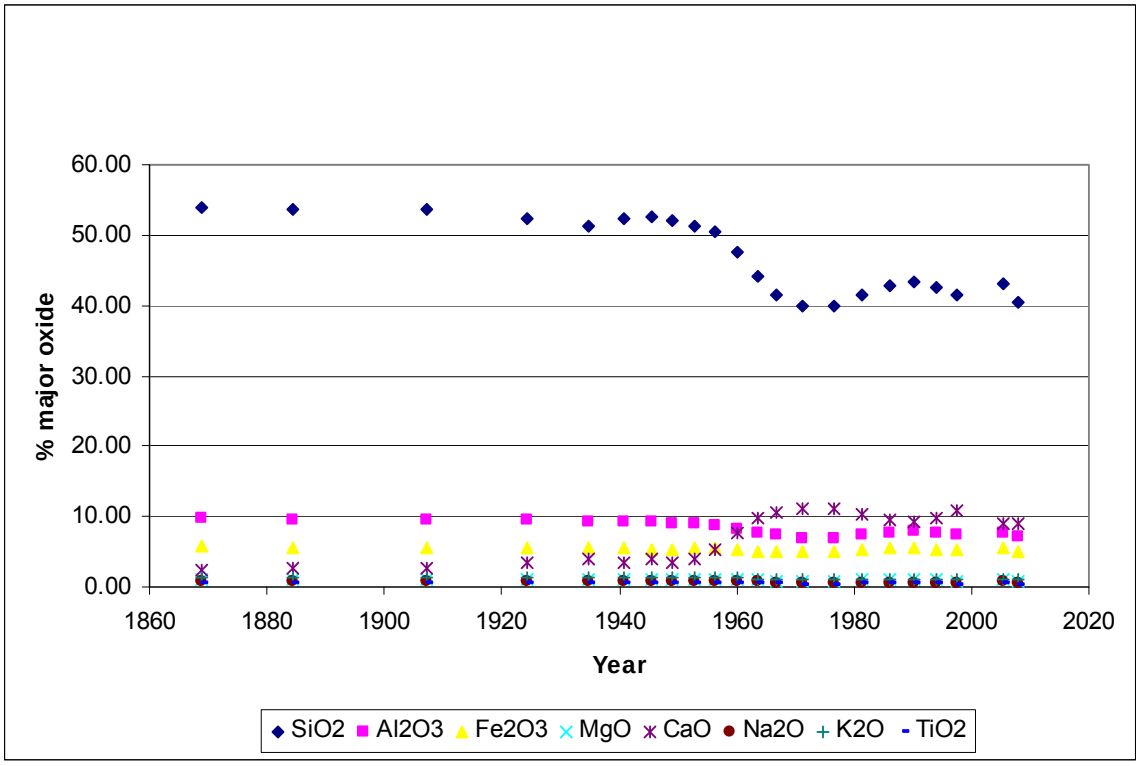

Figure 6. Temporal changes in major oxide composition in the sediment core CL-C

The change in mineralogy with depth of the Core CL-C is depicted in Figure 7. The most notable difference in mineralogy between the shallower (less than about 6 cm) and the deeper sediments is the abundance of calcite and ankerite (?) in the upper sediments. Based on the relative peak intensities, the deeper sediments contain slightly higher amounts of the common mineral components, which include in order of decreasing abundance, quartz, chlorite, feldspars, pyrite, mica and trace hornblende. The calcite peaks (not all labelled in Figure 7) are sharp, indicating that the mineral is well crystalline. However, the suspected ankerite (?) are characterized by broad peaks, indicating that it is a poorly crystalline carbonate phase, which may contain other elements such as Zn and Mn in solid solution. The formation of both calcite and ankerite could result from water treatment or discharge of process water to the lake. Due to overlapping reflection peaks, the possible occurrence of poorly crystalline manganese oxides in

the shallower sediments cannot be fully discerned. Overall, the observed changes in mineralogy with depth agree with the major and trace element profiles. They reinforce the observation that physical sedimentation dominated in the early years, then chemical sedimentation increased around 1960.

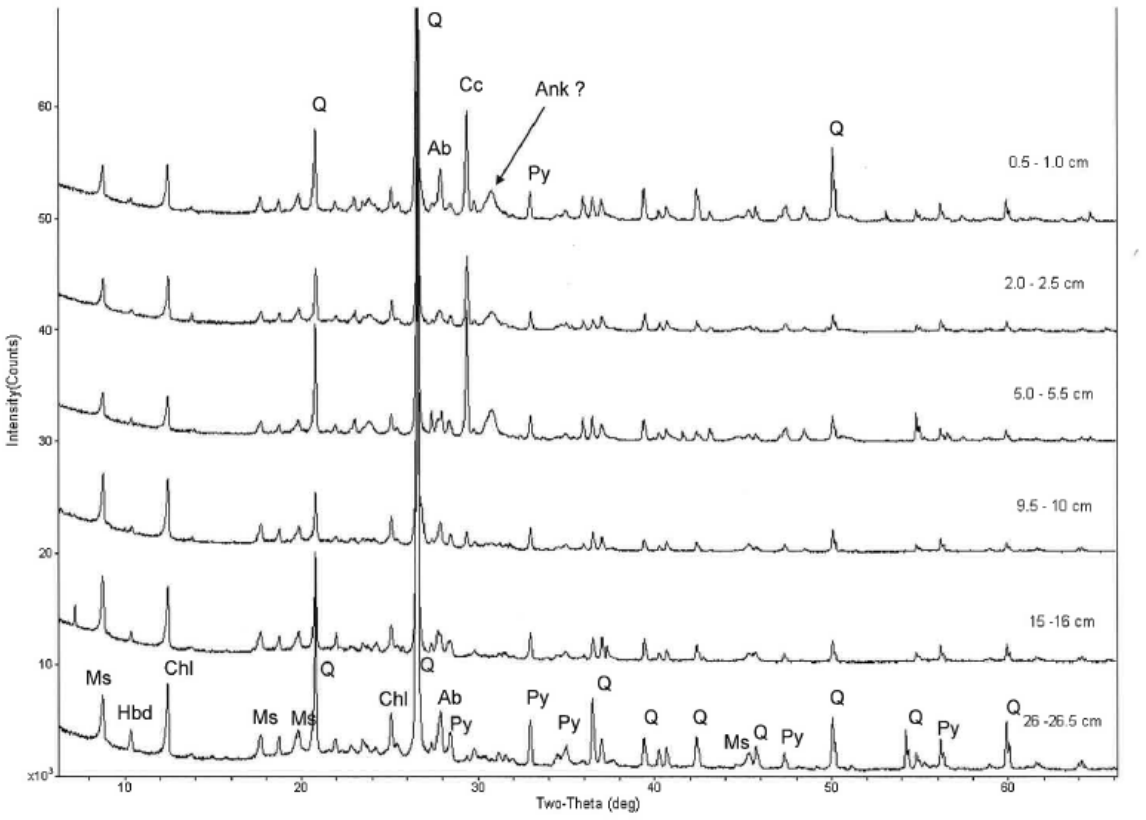

Figure 7: Variation in mineralogy with depth in the sediment core CL-C (Acronyms: Q – quartz; Ab- albite; Cc – calcite ; Py – pyrite; Chl – chlorite; Ms – muscovite ; Hbd - hornblende)

Geochemistry and Mineralogy of Other Cored Sediments

The concentrations of selected heavy metals, including Fe, Mn, Pb, Ti and Zn, in other sediment samples collected from Christal Lake and farther downstream are tabulated in Appendix 1. These results represent semi-quantitative measurements with a hand-held, field X-Ray fluorescence (XRF) spectrometer which may not be as accurate as the core CL-C results.

However, they are considered to be of sufficient quality to reflect the relative abundance of the pertinent elements in the sample set. General observations that can be made from the tabulated data in Appendix 1 include the following:

1. The sediments do not share similar chemistry, but vary in composition with both location and depth.
2. Notable Pb concentrations (0.04 – 0.48 %) are detected only in Christal Creek sediments sampled at a short distance from the outlet of Christal Lake; the location suggests that the Pb is sourced from the Mackeno tailings nearby.
3. With a few exceptions, Zn appears to be more concentrated in the near surface sediments than at depth, but its correlation with Mn is not as clear as in the finely segmented CL-C core.
4. Elevated Mn and Zn concentrations are particularly notable at all depths in the sampled Christal Creek sediments and, to a lesser extent, in the shallower lake sediments at three locations (CL-B, CL-C, CL-1) which are susceptible to impacts from the Galkeno 300 treated discharge overland flow, the Galkeno 900 treated discharge and the Mackeno tailings (see Figure 2 for location).

The relationship between sediment Mn and Zn is further explored in Figure 8. Two linear trends of variation of total Zn with Mn content are apparent, one characterized by Mn>Zn and the other by Zn>Mn. Most of the lake and creek sediments sampled at stations greater than about 60 m from the old Mackeno tailings site fall close to trend line a (Figure 8) with a Mn/Zn weight ratio of about 5 to 1. On the other hand, stream sediments from sampling stations closest to the Mackeno tailings (especially CCR-2 and -3, Figure 2) define a line with a Zn/Mn weight ratio of about 1.4 to 1 (trend line b, Figure 8). In addition to XRD analysis, selected samples from both series were examined with scanning electron microscopy to identify the mineral hosts of these two metals.

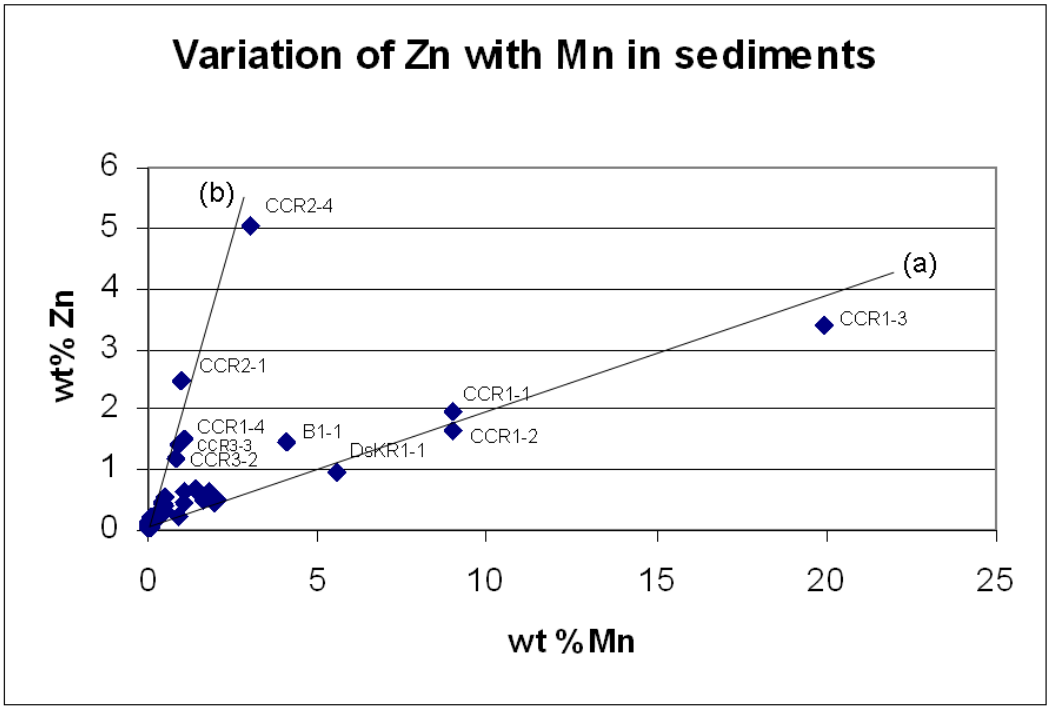

Figure 8: Variation of Zn with Mn in the Christal Creek and Christal Lake sediments (excluding data from core CL-C for age dating, which has been presented in Figure 5). See text for a description of trend lines (a) and (b).

Figure 9 shows the X-ray diffractograms of three selected samples which follow trend line (a) identified in Figure 8. Although they share a similar Mn/Zn weight ratio, the three samples differ drastically in mineralogical composition. The top-most sample of the lake core B (B1-1, 0-10 cm) is dominated by quartz with subordinate amounts of gypsum and a carbonate solid solution akin to kutnohorite [$Ca(Mn,Mg,Fe,Zn)(CO_3)_2$], as well as minor amounts of chlorite, sericite and K-feldspar. In addition, the abundance of broad peaks throughout the scanning range suggests the presence of poorly crystalline phases, the true identity of which cannot be unambiguously established by powder X-ray diffractometry. The top segment of the sediment core at site CCR-1 (CCR1-1, 0-9 cm) is dominated by quartz and ankerite (with an ideal chemical formula of $Ca(Fe,Mg)(CO_3)_2$ but may contain some Mn and Zn in solid solution) with lesser amounts of manganese-rich siderite [$(Fe,Mn)CO_3$], feldspars, chlorite, sericite and trace gypsum. Some forms of amorphous manganese oxide/hydroxide may also be present. The third

segment of the same core (CCR1-3, 18-27 cm), on the other hand, is dominated by quartz and an unidentified manganese oxide/hydroxide with minor amounts of gypsum, feldspars, Mn-rich siderite, chlorite and sericite. As no discrete Zn-mineral is found, it is speculated that most zinc in these samples is hosted by amorphous manganese oxide/hydroxide and/or occurs in the carbonate solid solutions. This possibility is further explored with scanning electron microscopy.

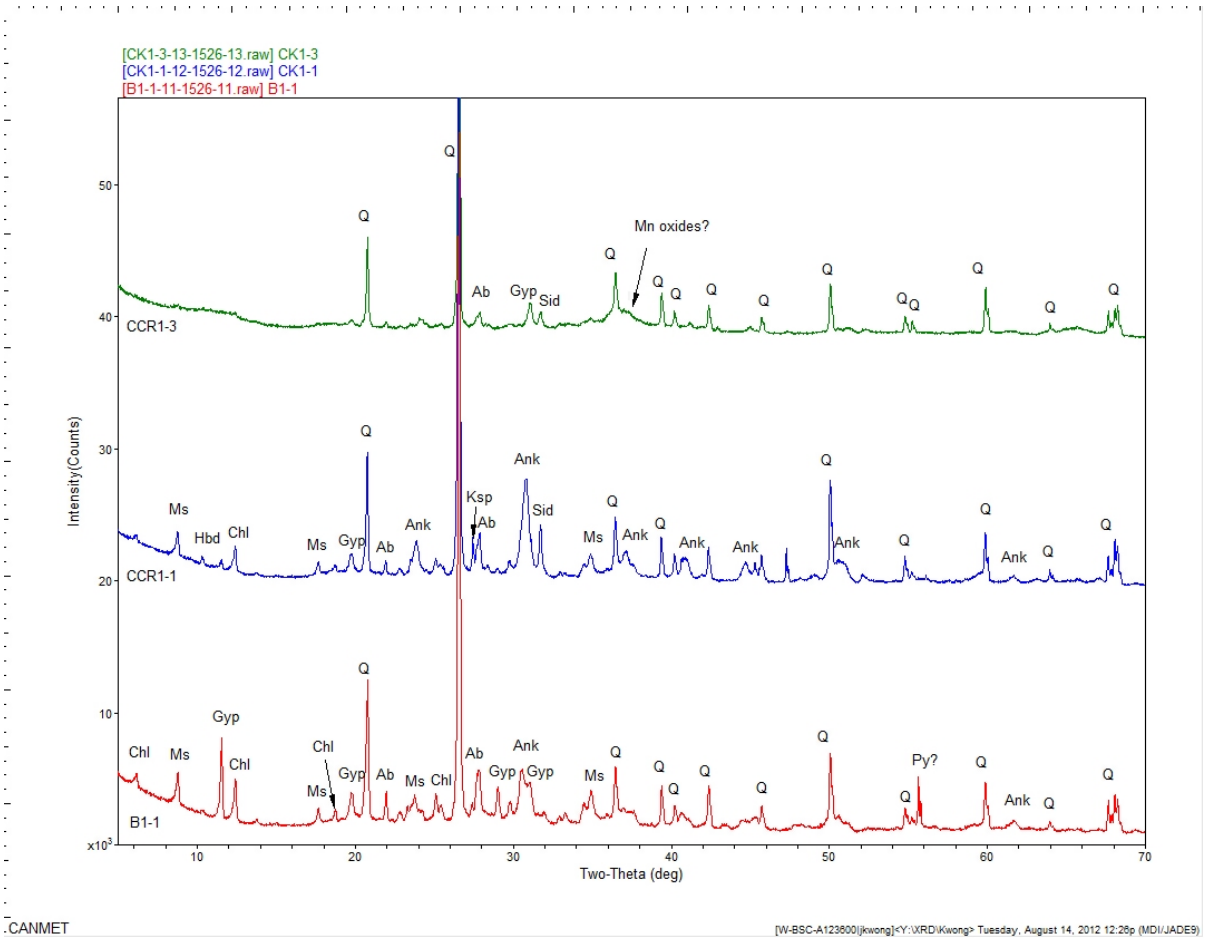

Figure 9: X-ray diffraction patterns of three selected samples with Mn/Zn >1 by weight. (Abbreviations: Ab = albite; Ank = ankerite/kutnohorite, Chl = chlorite; Gyp = gypsum; Hbd = hornblende; Ksp = K-feldspar; Ms = muscovite/sericite; Q = quartz; Sid = siderite)

Figure 10 shows an X-ray map (top) and a back-scattered electron image (bottom) of a section of a grain-mount sample of the sediment segment B1-1, acquired upon examination of the sample at a relatively low magnification (200X). The identification of the various solid phases labelled in

the backscattered electron image is based on the bulk XRD analyses, co-existence of various elements at the same grains as is evident from the X-ray maps and spot EDX analyses (results not shown). The primary focus of the SEM/EDX analysis was to identify authigenic secondary minerals and the Zn-bearing phases. As such, although primary minerals such as quartz, plagioclase (albite) and chlorite were often encountered, they were not analyzed in detail and the corresponding grains were not labelled in most images. However, selected grains of muscovite/sericite (Ms, which appears to occur both as a primary and secondary mineral based on their morphology) and potassium feldspar (Ksp, a primary mineral), are labelled in Figure 10 for comparative purposes. From the data shown in Figure 10, the following observations can be made:

1. Whereas Zn correlates well with Mn, it is hosted by kutnohorite (marked as Kut? in the bottom image of Figure 10) and jarosite (jar+Zn) in addition to manganese ± iron oxides/hydroxides.

2. Zn-bearing Mn oxides/hydroxides rarely occur as isolated grains but in agglomeration with Fe oxides/hydroxides giving rise to 20-40 μm aggregates either enriched in Fe (FeMnO+Zn) or Mn (MnFeO+Zn), but both are Zn-bearing.

3. The abundance of gypsum (gyp) appears to be significantly less than what is suggested in the XRD analysis of the bulk sample. However, the grain-mount sample for SEM examination represents a tiny subsample of the original, unprocessed sediment instead of a larger subsample pulverized for XRD analysis. As such, the apparent inconsistency could be an artefact of sample heterogeneity. Alternatively, preferred orientation of gypsum in the XRD sample could have resulted in higher reflection peaks that are not representative of its actual abundance.

4. As suggested by their morphology (angular instead of globular), a few micro-size sphalerite (sph) grains detected in the loose-grain mount are likely detrital rather than authigenic (i.e. precipitated in situ) in origin.

The observed occurrence of jarosite in sediment B1-1 is unexpected because the mineral does not normally form under near-neutral pH conditions. However, the concomitant concentration of Fe, S, K and Al in the agglomerated grain attached to one end of a diatom sheath (Figure 10, top) provides strong evidence that it could be hydronian jarosite [$(K,H_3O)Fe_3(SO_4)_2(OH)_6$] with some Al substituting for Fe, which is common in a jarosite-allanite solid solution series. A micro environment enriched in organic acids derived from decaying organic matter might have facilitated its precipitation. In any case, as shown by the concentration of Zn and minor Mn in the same grain, the mineral appears to be an efficient scavenger for Zn. It should be noted that jarosite is a rare mineral in the samples examined; it was only observed once in B1-1. Overlapping reflection peaks with gypsum would hamper its identification by powder X-ray diffractometry, even if it occurs in greater abundance in the sample. The persistence of jarosite and some detrital sphalerite in the surface lake sediment B1-1 suggests that even though they may not be thermodynamically stable, slow reaction kinetics under the prevailing site conditions have facilitated their preservation in the sediment.

Selected results obtained upon examination of the creek sediment sample CCR1-3 under a scanning electron microscope are depicted in Figures 11 and 12. Figure 11 shows a backscattered electron image of a segment of a loose-grain mount and the corresponding X-ray maps of Al, Si, S, K, Ca, Mn, Fe and Zn. It is worth noting that Fe also occurs in the secondary Mn-oxides, which evidently incorporate Zn in their geochemistry (Figure 11, top image). More pyrite and sphalerite are encountered in this sample than in the lake sediment B1-1. Their well crystalline form indicates that they are primary sulphide minerals. The proximity of the sampling station CCR1 to the former Mackeno tailings impoundment suggests that the latter could be a source of the sulphides. In addition, minor amounts of gypsum were detected in sample CCR1-3. They usually occur in combination with Fe/Mn oxides (an example is shown in Figure 12). Their morphology suggests that they are authigenic in origin. Although the sample was taken at moderate depth (18-27 cm), the prevalence of authigenic Mn/Fe oxides and gypsum provides evidence that sulphate reduction is not occurring.

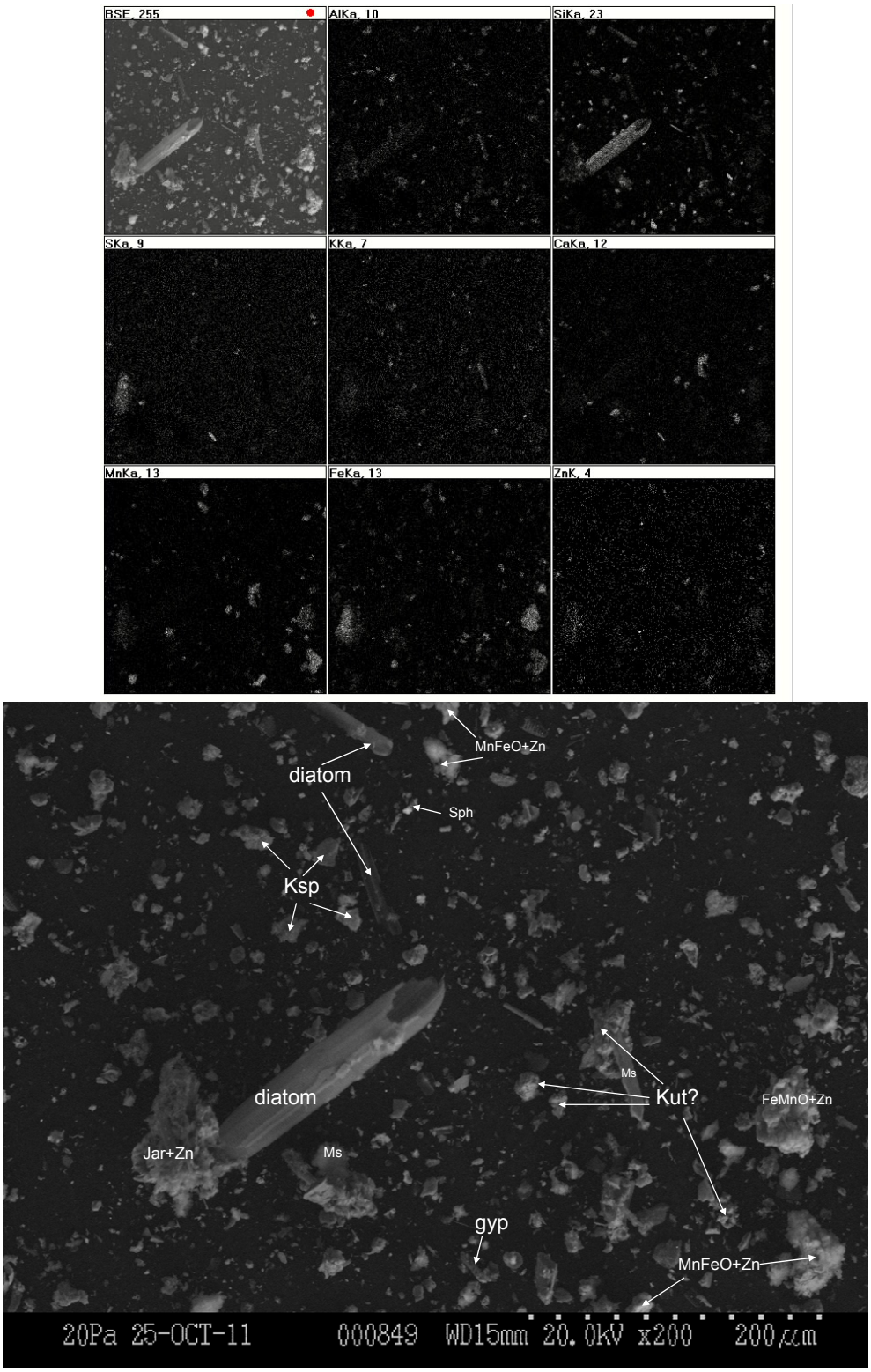

Figure 10: An X-ray map (top) and an enlarged backscattered electron image (bottom) of a section of a grain-mount of sample B1-1 taken under at low magnification (200X). See text for an explanation of abbreviations used.

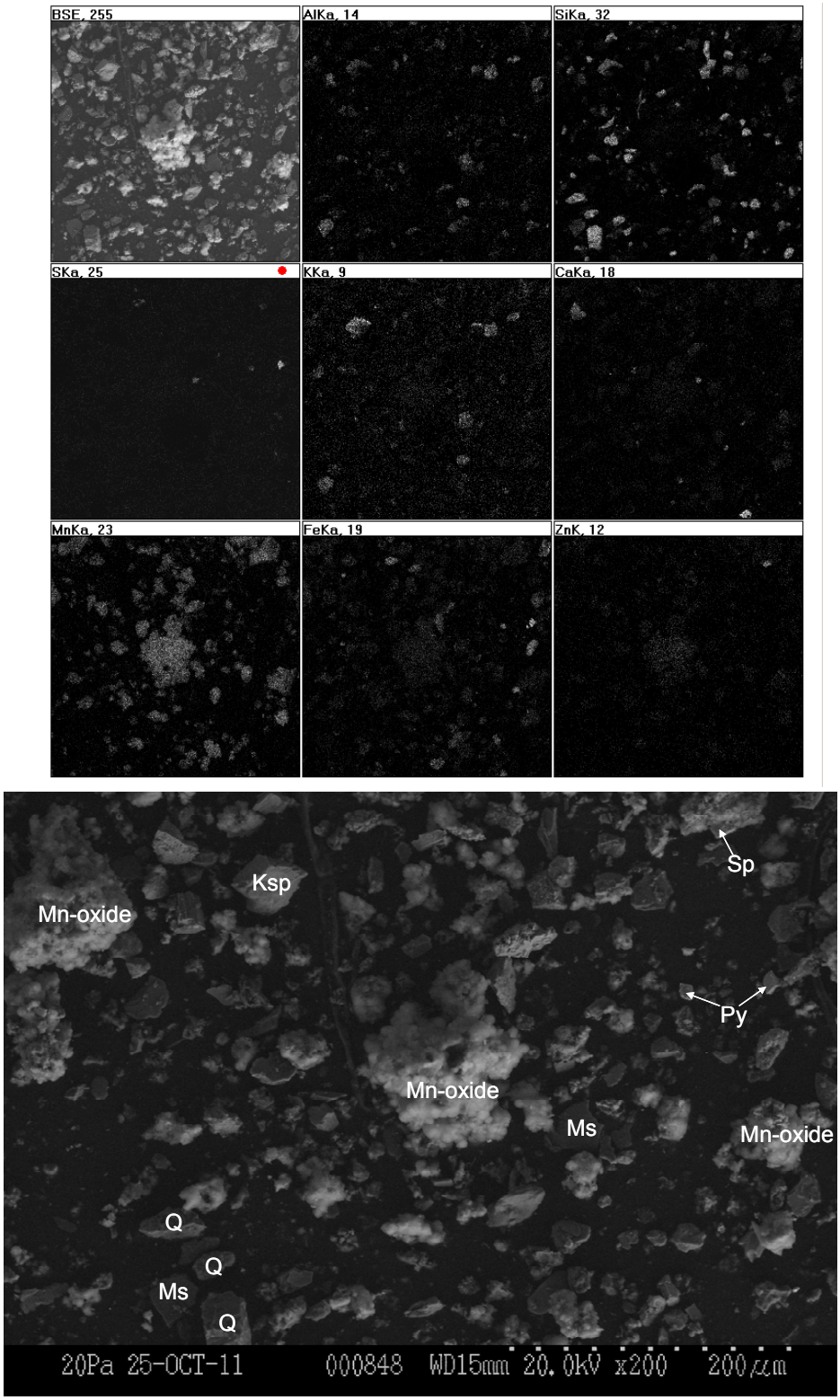

Figure 11: X-ray maps (top) and a backscattered image (bottom) of a loose-grain mount of sediment CCR1-3 at low magnification (200X). Abbreviations: Ksp = K-feldspar, Ms = muscovite/illite, Py=pyrite, Q=quartz, Sp=sphalerite.

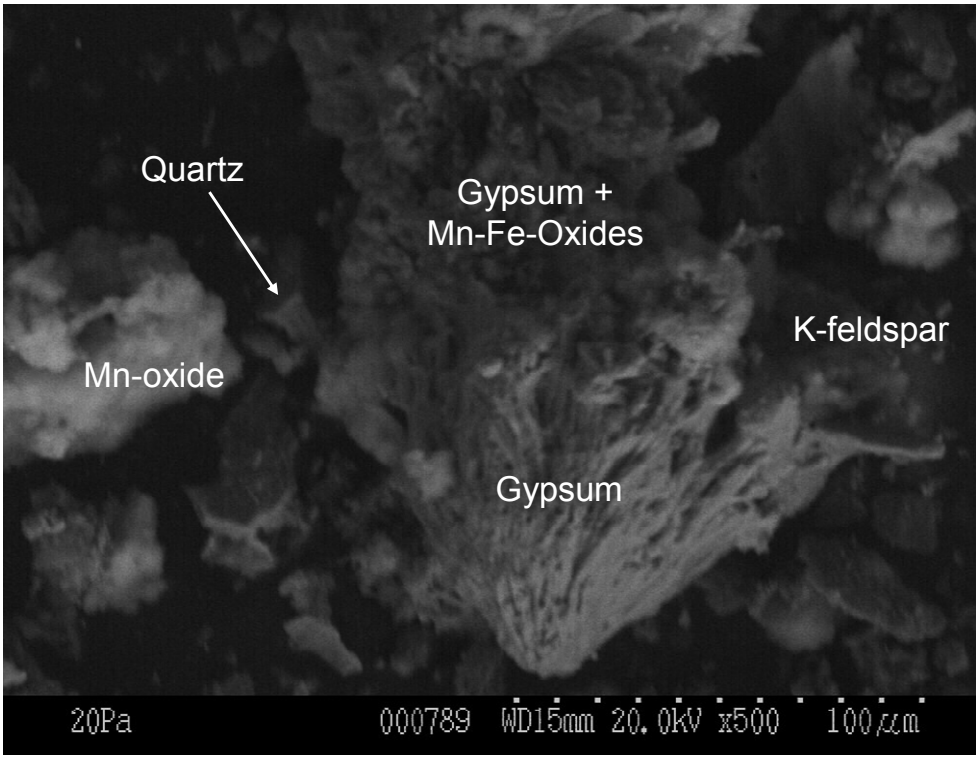

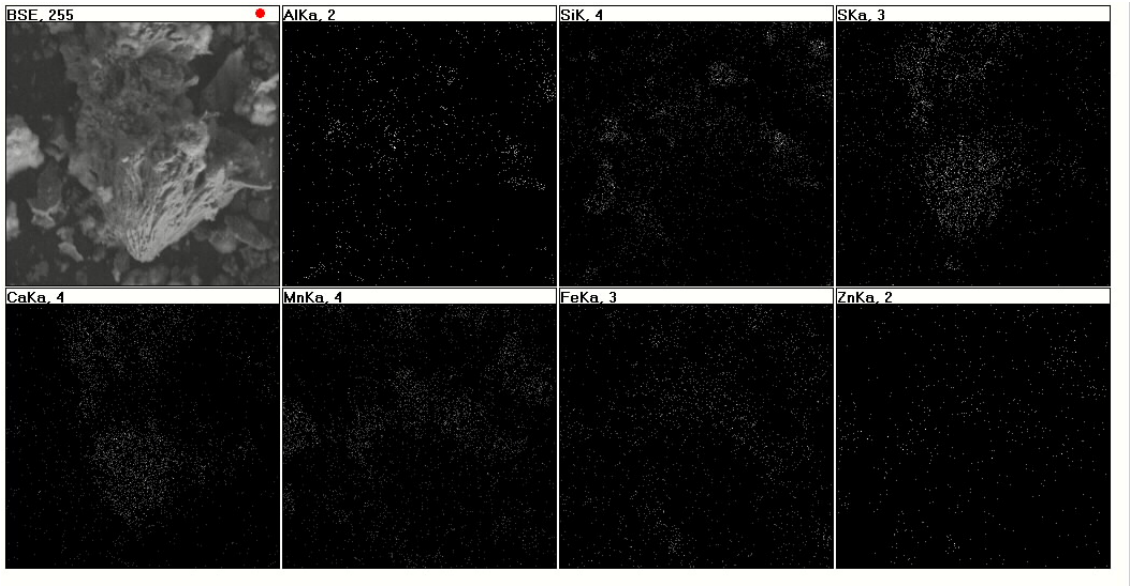

Figure 12: Backscattered electron image of gypsum (top) in a loose-grain mount of sample CCR1-3 with the corresponding X-ray maps (bottom).

The X-ray diffractograms of three selected samples with Mn/Zn<1 by weight (trend (b) in Figure 8) are shown in Figure 13. Compared to those of the samples with a higher Mn/Zn weight ratio, these diffraction patterns generally have a lower background and sharper reflection peaks, indicating the presence of mostly crystalline constituents. The surface segment of the sediment core (CCR2-1; 0-9 cm) taken at the sampling station CCR2 is dominated by quartz with minor amounts of plagioclase, chlorite, ankerite, muscovite, hornblende and possibly some sphalerite. However, the deepest segment of the same core (CCR2-4; 27-36 cm) consists of quartz, sphalerite, siderite and a trace amount of muscovite/sericite. Such a mineral assemblage is suggestive of tailings from the former Mackeno mine. This is confirmed by the identification of trace amounts of other primary sulphide minerals including galena, pyrite and possibly mackinstryite [$(Ag,Cu)_2S$] upon examination of another subsample with scanning electron microscopy (Figure 14). A detailed review of the d-spacings of the identified siderite suggests that it could also be oligonite, $Fe(Mn,Zn)(CO_3)_2$, which is essentially a zinc-bearing solid solution between siderite ($FeCO_3$) and rhodochrosite ($MnCO_3$). If this is proved to be true, then primary siderite/oligonite can also be a minor source of zinc in addition to sphalerite in the mining district. The mineralogy of the mid-depth core segment (CCR3-2; 10-20 cm) from a station farther downstream is intermediate between CCR2-1 and CCR2-4, with quartz >> sphalerite ≥ oligonite/siderite ≥ plagioclase > K-feldspar > chlorite > hornblende > trace gypsum. Based on the mineralogy of these samples, it is apparent that the key parameter that controls the variation in the weight ratio of Mn/Zn in a stream or lake sediment is the relative abundance of detrital primary sphalerite versus secondary, authigenic manganese oxides/hydroxides. For Mn/Zn<1 by weight to occur, the prevailing amount of detrital sphalerite has to exceed that of authigenic manganese oxides/hydroxides.

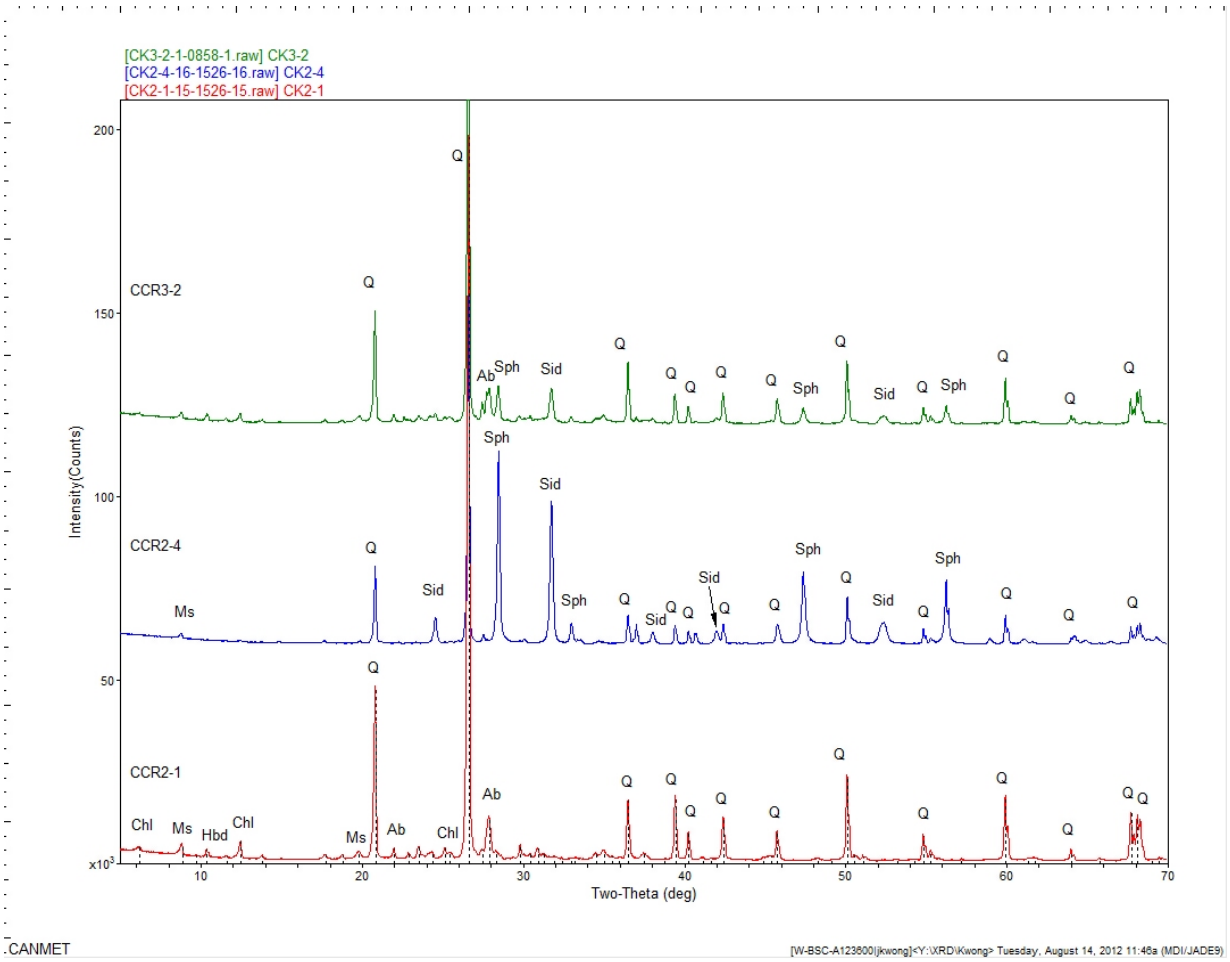

Figure 13: X-ray diffractograms of three sediment samples with Mn/Zn <1 by weight. (Abbreviations used are the same as in Figure 11, except that Sph = sphalerite)

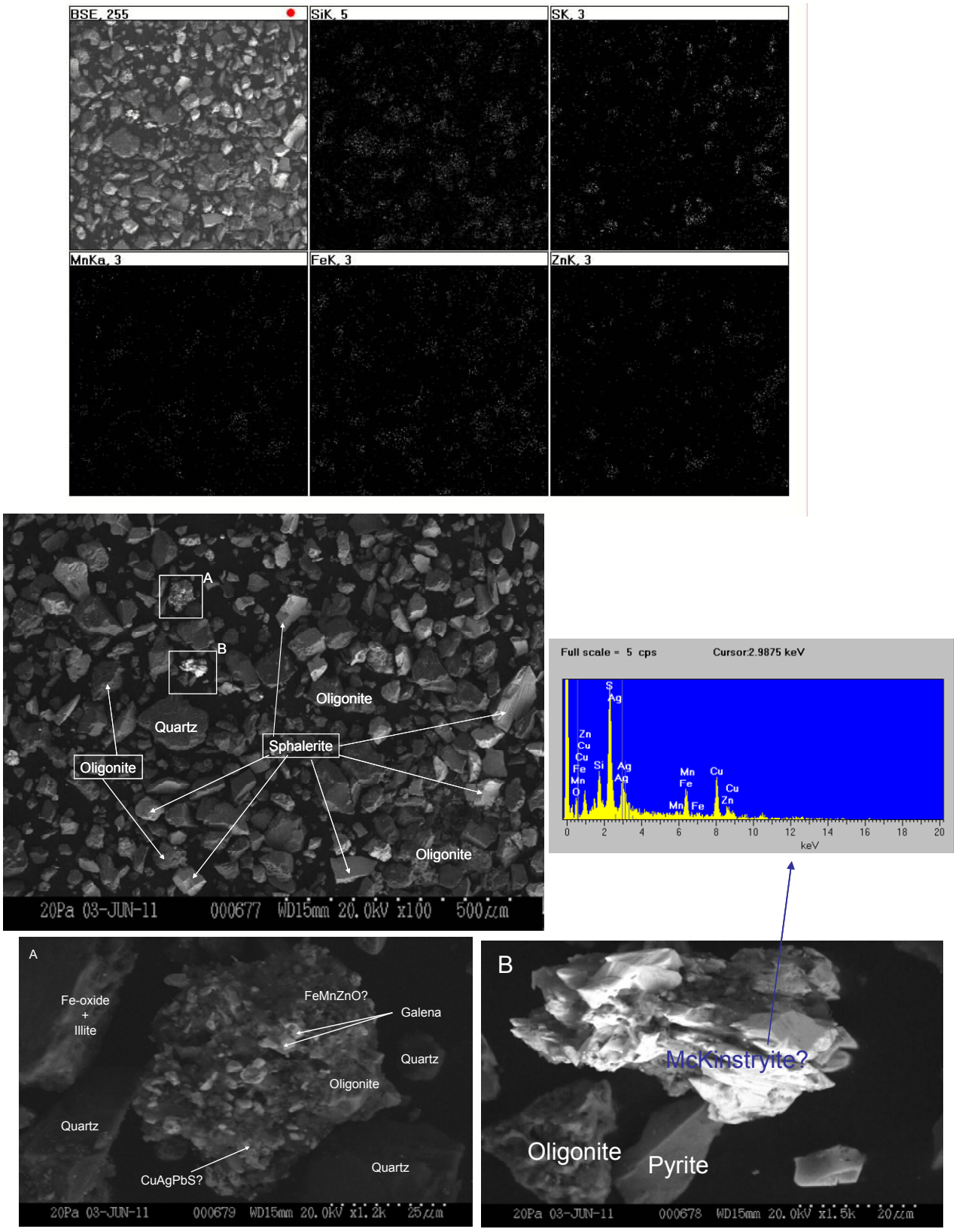

Figure 14: X-ray maps (top) and their interpretation for sample CCR2-4.

Water Chemistry

Summer 2008 Data

Table 2 shows selected water chemistry at a few sediment sampling stations in Christal Lake and a couple of the downstream stations sampled in the summer of 2008 (with data arranged in a downstream direction). The lake water was generally uniform in pH (7.4-7.7), dissolved Fe (0.03-0.06 mg/L) and dissolved Zn (0.05 mg/L). While dissolved Mn (0.09-0.28 mg/L) appeared to increase in a downstream direction, the slight variation in dissolved sulphate (194-245 mg/L), Si (2.46-2.68 mg/L) and Ca (87.3-101 mg/L) content was more randomly distributed. With a few exceptions, dissolved concentrations for Ca, Mn, and Si were similar to the total concentrations, indicating that suspended particles did not contribute much to the overall concentrations of these metals in the collected water samples. On the other hand, as reflected by the significantly higher total concentrations, suspended particles made up a significant portion of the detected Fe and Zn.

Near the lake outlet, a slight increase in Ca, Mn and total Zn concentrations was apparent, likely reflecting the impact of discharge of treated effluent from Galkeno 900. Between the lake outlet and the sampling station upstream of the Silver Trail Highway (DS Keno Rd), there was evidently additional input of both dissolved and total Zn (0.05-0.24 mg/L and 0.13-0.34 mg/L, respectively) to the drainage system. In contrast to sulphate, Ca, Fe and Mn, the Zn was not attenuated to levels at or below those measured in Christal Lake at the last sampling station upstream of the South McQueston River. However, there was insufficient data between the two sampling stations to reveal if there were additional local sources of Zn along the flow path.

Table 2: Selected water chemistry in the Christal Lake/Creek drainage system in summer 2008

Station (Sampled 080827)	Field pH	Sulphate (mg/L)	Ca (mg /L)		Fe (mg /L)		Mn (mg /L)		Si (mg /L)		Zn (mg /L)	
			dissolved	total	dissolved	total	dissolved	total	dissolved	total	dissolved	total
CL-G	7.68	232	94.8	107	0.03	0.18	0.09	0.14	2.46	2.58	0.05	0.08
CL-H	7.49	194	87.3	95.6	0.06	0.27	0.20	0.20	2.59	2.62	0.05	0.10
CL-C	7.68	236	91.6	98.2	0.03	0.16	0.14	0.16	2.50	2.51	0.05	0.09
CL-D	7.65	231	89.3	97.4	0.04	0.32	0.21	0.24	2.60	2.72	0.05	0.09
CL-A	7.54	237	101	101	0.03	0.29	0.24	0.27	2.70	2.63	0.05	0.09
CL-B	7.57	236	94.2	102	0.04	0.30	0.22	0.26	2.60	2.62	0.05	0.09
CL-3	7.46	223	93.5	93.9	0.04	0.31	0.26	0.26	2.62	2.66	0.05	0.09
CL-1	7.41	245	98.0	109	0.03	0.20	0.27	0.27	2.73	2.68	0.05	0.10
CL-Outlet	7.45	267	108	123	0.03	0.33	0.28	0.26	2.68	2.74	0.05	0.13
DS Keno Rd	7.54	254	105	119	0.05	0.19	0.25	0.28	2.70	2.87	0.24	0.34
CCr u/s South McQueston River (sampled 080909)	8.15 (lab)	157	82.4	84.8	0.05	0.15	0.10	0.11	2.74	2.65	0.18	0.22

The rapid distilled-water leach test results for all the segmented sediment cores (from both Christal Lake and Christal Creek immediately downstream) are tabulated in Appendix 2. Key observations that can be made from these data include the following:

1. There is a random, high variation of various elements with depth, reflecting the heterogeneous mineralogical composition of the sediments which ultimately controls the local pore water chemistry.

2. The sediment leachates, which may be interpreted to be reflective of the porewater composition, are enriched in various elements compared to the overlying lake water. Whereas the enrichment in dissolved Ca, S and Si generally does not exceed an order of magnitude, the increase in some metals such as Cd, Cu, Fe, Mn, Pb and Zn often amounts to several orders of magnitudes. This is especially evident in leachates which were brownish in colour, reflecting the presence of dissolved organics. This in turn indicates that dissolved organic-metal complexes occur in some of the sediment porewaters.

3. The random variation of various elements with depth, which may differ in concentrations by orders of magnitudes relative to the overlying lake water, is

evidence that there is little vertical movement of water through the sediments into Christal Lake. Metal efflux from sediment porewater to the lake can occur only through diffusion, which is apparently insignificant. Christal Lake thus serves as a sink rather than a source for most metals, including Cd, Fe, Mn and Zn.

4. Similar observations with the creek sediment leachates suggest that the submerged sediments are not a source of metals to the creek water, at least during the time of sampling. The higher dissolved and total zinc concentrations in the creek compared to the lake water (Table 2) indicate an external source of the metal to the drainage system past the lake outlet.

Seasonal Changes in Water Chemistry

Given that Christal Lake is relatively shallow (maximum 2 m in depth) and often freezes to a depth of 40-50 cm in winter, it is expected that the lake water chemistry will change under an ice cover. Table 3 compares some selected lake water chemistry data at several sampling sites in March and August 2008, representative of winter and summer conditions, respectively. In addition to temperature, there were significant increases in pH, ORP and dissolved oxygen (except the March 29 measurement for CL-A, which is suspect) in the summer (August) versus winter (March). In contrast, specific conductance, dissolved sulphate, total dissolved solids (TDS) and dissolved and total concentrations of both Mn and Zn were higher during March under an ice cover. In addition, most of the measurements for total suspended solids (TSS) were higher in March than in August. Since it is unlikely that any groundwater movement could occur during the winter months, the increases in dissolved sulphate, TDS and hence specific conductance must be due to the concentration effect in the remaining water as the ice cover started to form. However, the higher concentrations of Mn and Zn could result from a combination of two processes, namely, partial freezing of the lake water and dissolution of Zn-containing manganese oxides/hydroxides which were either formed in-situ or transported to the lake during the open-water months. Conversely, the reduced

ORP and DO measurements in the winter reflect consumption of dissolved oxygen by decaying organic matter in the lake, creating redox conditions favourable for the reduction of manganese oxides but not ferric iron and sulphate (Borch et al., 2010). Thus Mn and Zn remobilization is effected under an ice cover.

Table 3: Comparison of selected winter and summer water chemistry in Christal Lake

Station/ sampling dates	Temperaure (degree C)	Specific conductance (µS/cm)	Field pH	Field ORP (mV)	Dissolved Oxygen (mg/L)	Sulphate (mg/L)	TDS (mg/L)	TSS (mg/L)	Mn (mg/L) diss./total	Zn (mg/L) diss./total
CL-1										
08-03-29	0.2	1610	6.51	n/a	1.08	645	1330	24	6.29/6.59	0.15/0.37
08-08-27	9.6	630	7.41	88	9.97	245	500	5	0.27/0.27	0.05/0.10
CL-A										
08-03-29	0.7	3910	6.30	41	9.27	590	949	5	0.91/0.73	0.18/0.38
08-08-27	9.7	610	7.58	88	9.99	237	486	5	0.24/0.27	0.02/0.09
CL-B										
08-03-29	0	1660	6.61	21	3.01	1090	1760	5	4.51/5.20	1.39/1.62
08-08-27	9.6	600	7.57	66	9.98	236	490	5	0.22/0.26	0.05/0.09
CL-C										
08-03-29	0.3	810	6.95	-38	2.57	306	595	87	0.16/1.56	0.21/1.01
08-08-27	9.9	590	7.68	87	10.4	236	472	5	0.14/0.16	0.05/0.09
CL-D										
08-03-29	0.1	820	7.04	-16	3.19	310	600	23	0.24/0.43	0.23/0.40
08-08-27	9.6	580	7.65	93	10.3	231	480	5	0.21/0.24	0.05/0.09
CL-G										
08-03-29	0.1	1510	6.88	n/a	0.84	243	1130	47	1.70/1.98	0.14/0.40
08-08-27	10.2	610	7.68	126	10.1	232	490	5	0.09/0.14	0.05/0.08
CL-H										
08-03-29	0.1	810	7.07	-15	3.05	311	588	10	0.17/0.28	0.20/0.20
08-08-27	8.8	570	7.49	103	10.2	194	453	5	0.20/0.20	0.05/0.10

*n/a = not available

In detail, the releases of Mn and Zn in winter do not appear to correlate well with each other. This is further complicated by the heterogeneous composition of the water column as evidenced by the high variation of all measured parameters across the lake (Table 2), indicating that it is not well mixed in any season of the year. The seasonal behaviour of Mn and Zn was further investigated along Christal Creek using available data (to the end of 2010) from three selected monitoring sites (Figures 15 and 16) to demonstrate the temporal changes of dissolved Mn and Zn in the drainage system. The data (unpublished) form part of the data set compiled by the Access Consulting Group to inform on-going reclamation activities in the Keno Hill mining district.

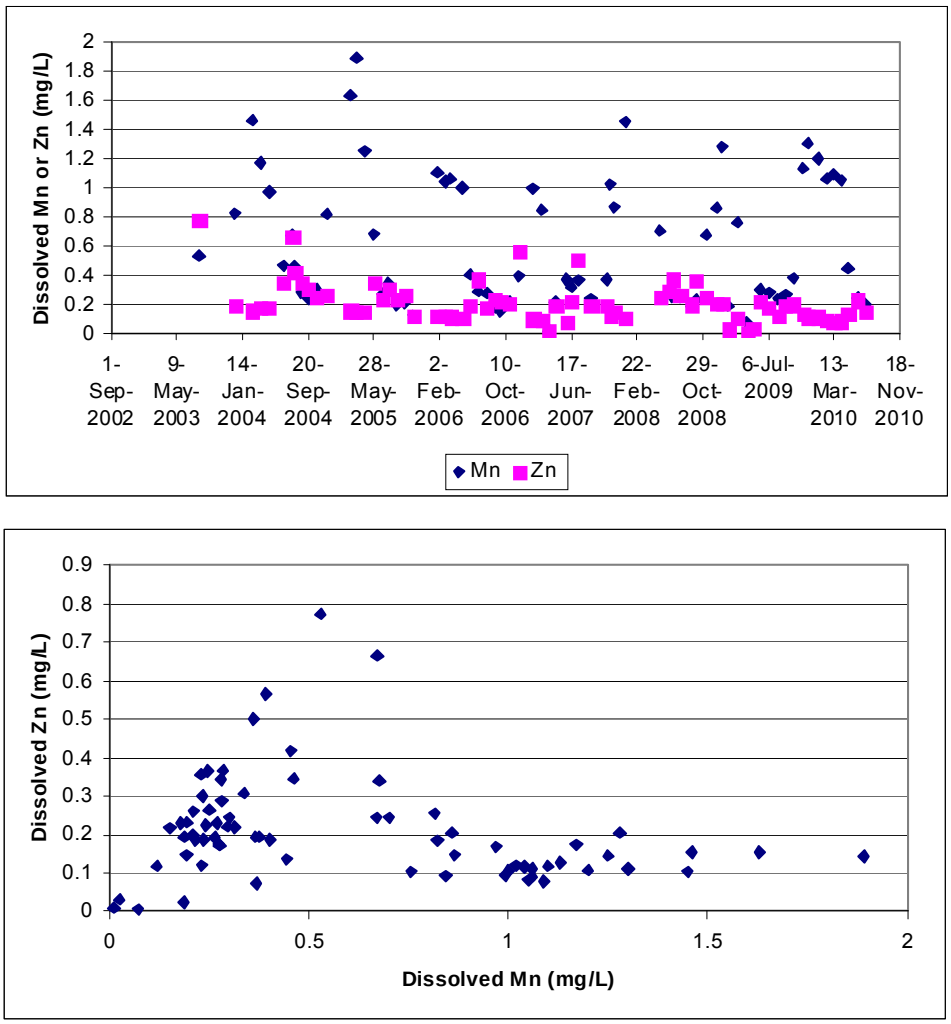

Figure 15: Temporal variation of dissolved Mn and Zn at monitoring location KV-6 (Christal Creek at Silver Trail Highway) and their mutual correlations (lower plot).

The variation of dissolved Mn and Zn from 2002 to 2010 at Christal Creek near the Silver Trail Highway (monitoring point KV-6) is shown in the upper plot of Figure 15. While a gradual decrease of the two metals with time is apparent at KV-6, dissolved Mn exhibits a different seasonal variation pattern compared to dissolved zinc. The Mn tends to peak during the winter months (November – April), whereas the Zn peaks during the summer months, leading to an overall poor correlation between the two parameters (Figure 15, lower plot). Excluding a few "suspect" data in the raw data set, the seasonal statistics of the two dissolved metals are calculated and presented in Table 4. It is clear that Mn and Zn behave differently under ice-covered conditions.

Table 4: Seasonal statistics of dissolved Mn and dissolved Zn at Christal Creek by the Silver Trail Highway (KV-6) for the monitoring period 2002-2010.

	Dissolved Mn (mg/L)		Dissolved Zn (mg/L)	
	Nov-Apr	May-Oct	Nov-Apr	May-Oct
Number of analyses	28	43	28	43
Range	0.217-1.89	0.119-0.702	0.078-0.256	0.072-0.774
Median	1.06	0.281	0.124	0.224
Mean	1.07	0.320	0.140	0.265
Standard deviation	0.317	0.133	0.048	0.141

The following interpretation is proposed for the seasonal difference in the behaviour of Mn and Zn as demonstrated in Figure 15 and Table 4. Under open-water conditions, manganese oxides and/or hydroxides precipitates readily form, resulting in low concentrations of dissolved Mn at the sampling site. Some of the zinc is co-precipitated with the manganese oxides/hydroxides. In the winter time, slightly reducing conditions develop under the ice cover. As a result, some of the exposed (i.e. not yet covered by other sediments) manganese oxide precipitates undergo reductive dissolution, and give rise to the increase in dissolved Mn concentration. However, the co-precipitated Zn is immediately scavenged by another mineral, likely a secondary carbonate, upon its release from the dissolving manganese phase(s). The precipitation of an authigenic zinc-containing carbonate is made possible by the increasing ionic activities of the pertinent components in the aqueous phase concomitant with ice formation, which is more prominent volume-wise in Christal Creek than in Christal Lake, such that the solubility product of a precipitating mineral is exceeded. In the summer months, when the temperature rises and dilution increases, some of the exposed authigenic zinc-containing phase is redissolved, leading to a higher dissolved Zn concentration compared to that prevailing during winter.

The seasonal variation of dissolved Mn and Zn at two monitoring sites farther downstream, KV-7 (Christal Creek at Hansen Road) and KV-8 (Christal Creek upstream of South McQueston River), is shown in Figure 16. With a few exceptions (February-April 2004 at KV7; March-April 2004 and February 2008 at KV-8), there is a decreasing

trend in concentration of both metals from approximately 2004 at both monitoring sites. Dissolved Mn still peaks during winter months, but this is more pronounced at KV-7 than at KV-8. The seasonal variation pattern for dissolved Zn is unclear at both sites compared to that observed at KV-6. The dissolved Zn versus dissolved Mn plots for both sites show good correlation (Figure 16), suggesting that dissolution of Zn-containing Mn oxides/hydroxides is the primary source of the metals between the two monitoring sites. With continual attenuation through dilution and/or reprecipitation, the dissolved Mn concentration becomes very low near the confluence with the South McQuesten River, and is exceeded by dissolved Zn. A possible explanation is that a significant portion of the latter persists in the creek in the form of organic complexes or it is derived from a local source.

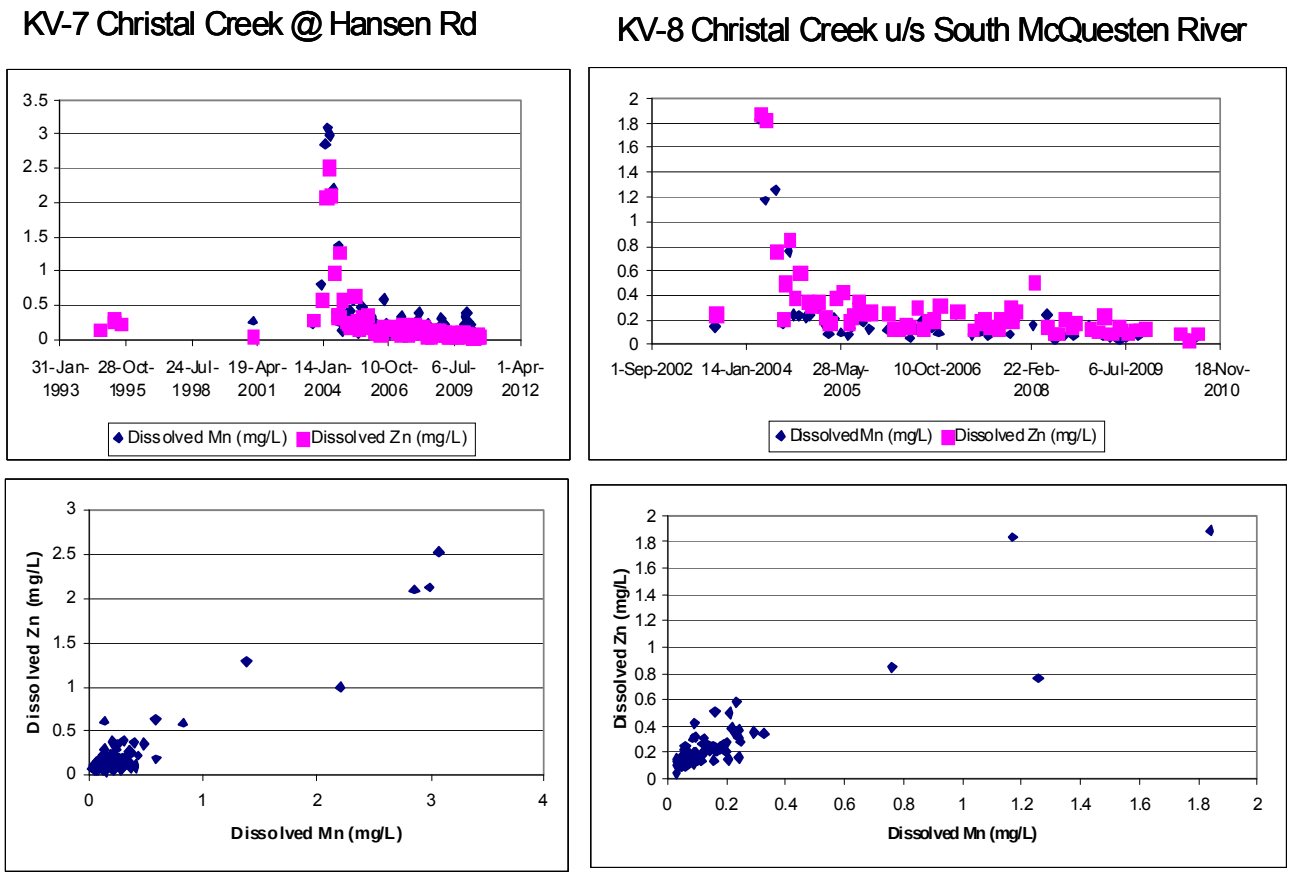

Figure 16: Temporal variation and correlation of dissolved Mn and Zn at sites KV-7 (Christal Creek at Hensen Road) and KV-8 (Christal Creek @ South McQuesten River). (Note difference in metal concentration scale in the plots for the two sites.)

It is not clear what caused the spikes of dissolved Mn and Zn in 2004 at KV-7 and in 2004 and 2008 at KV-8. They could have been generated by drainage disturbance from reclamation activities or intrusive sampling that occurred during that time. Various sampling campaigns have taken place recently in this area to inform the development of a decommissioning strategy for legacy sites in the historic mining district.

DISCUSSION

Using Christal Lake as a case study, the primary purpose of the current study is to determine the metal background and mobility in the historic Keno Hill silver mining district. Instead of relying on sophisticated analyses and modelling, this work focuses on deciphering what occurs in nature based on age dating of sediments in Christal Lake coupled with some simple geochemical and mineralogical analyses, and a thorough review of selected water monitoring data along the Christal Lake/Creek drainage system. Pertinent findings are discussed below.

Metal Background in Mineralized Terrains

Christal Lake lies among several past mines in the Keno Hill district and is the primary depository of erosion products and water draining from these deposits, both pre- and post-mining. Through age dating and the associated analyses, it is demonstrated that the lake sediment geochemistry closely correlates with the prevailing mining and reclamation activities. Thus the metal concentrations in the lake sediments deposited prior to the start-up of large-scale mining should reflect the natural metal levels in mineralized areas of the mining district. Based on this assumption and sediment analyses, the background levels of metals/metalloids of concern in sediment in the district are estimated at 344 ppm As, 6.0 ppm Cd, 52 ppm Cu, 30 ppm Ni, 43 ppm Pb and 796 ppm Zn. While the Cu, Ni and Pb levels are at the same order of magnitude as their crustal abundances (Levinson, 1980), both Cd and Zn are elevated by an order of magnitude and As by two orders of magnitude. In contrast, sediments in a stream draining non-mineralized terrains, such as

Star Creek, show As, Cd, Cu, Pb and Zn contents either below or comparable to their crustal abundances (Kwong et al., 1997). Given this large contrast in background metal levels in sediments from mineralized versus non-mineralized terrains, it appears impractical to define a common set of sediment criteria for permitting all new and pending mining operations, as well as for decommissioning old mine sites across the mining district. Site-specific guidelines that take the local natural background into account are more desirable. However, to justify setting site-specific guidelines, sufficient data must first be collected and interpreted to demonstrate their validity and relevancy before adoption.

Metal Mobility

This study investigated the main stretch of the Christal Creek/Lake drainage system (Christal Lake to Christal Creek at the Silver Trail Highway). The background sediment metal/metalloid contents in this area are elevated, relative to the corresponding crustal abundances and further enriched up to tenfold above the original concentrations for selected elements (notably Cd, Ni, Zn and, to a lesser extent, As) due to mining and reclamation activities. However, this enrichment is not proportionally reflected in the surface-water chemistry. This is particularly evident for As, the dissolved concentration of which hardly exceeds the analytical detection limit for most of the surface water samples analysed. However, the trace element levels in sediment porewaters as reflected by the leach test results are elevated, and vary greatly both vertically and horizontally, dictated in essence by the local sediment geochemistry and mineralogy. Higher total dissolved metal/metalloid contents are generally found in sediment porewaters which are apparently enriched in dissolved organics. Overall, with a few local exceptions, zinc is evidently the most mobile metal in the drainage system, subject to seasonal cycles of attenuation and remobilization but at decreasing concentrations downstream.

There are three possible reasons for the lack of correlation between sediment pore and surface water chemistry. First, once submerged under water, primary minerals containing potentially deleterious elements in the sediments are isolated from the weathering cycle,

limiting the release of elements of concern. As described in an earlier section, this occurrence was evident along the Christal Lake and Creek drainage system with the detection of fresh sphalerite, pyrite and minor galena and Ag-containing sulphosalts in many sediment samples, particularly those collected near the Mackeno tailings area. Second, metals transported in aqueous form may be depleted from the system through various mechanisms such as sorption onto various substrates, precipitation and co-precipitation as authigenic minerals, etc. Mineralogical and geochemical analyses documented in this study provide ample evidence of formation of secondary minerals (Fe and Mn oxides/hydroxides), carbonates (calcite, ankerite/kutnahorite) and sulphates (gypsum and jarosite), some of which are proven proficient zinc scavengers (e.g. Mn oxides/hydroxides). Third, whereas no primary or secondary minerals are absolutely insoluble and porewater in submerged sediments will eventually equilibrate with the surrounding minerals, leading to dissolved metal/metalloid concentrations much higher than those in the overlying water, diffusion of the dissolved metals/metalloids to the water cover is well known to be a very slow process. Covering of the authigenic minerals by continuous sedimentation, especially with inert materials, will further reduce the efflux of potentially deleterious metals/metalloids to the water column. Overall, although the Zn-bearing manganese oxides/hydroxides may re-dissolve under an ice cover in the winter months, the evidence strongly suggests that Christal Lake is a sink for zinc, rather than a source of zinc to the drainage system.

Permanency of Zinc Attenuation in the Christal Lake/Creek Drainage System

With few exceptions, the primary metal of concern in various drainage systems across the Keno Hill mining district is zinc (Interrologic Inc. 2012). In the Christal Lake/Creek system, zinc is the only trace metal invariably detected in every sediment and water sample analyzed. The following discussion on the longevity of natural attenuation along the drainage system thus focuses mainly on zinc.

Integrating the sediment mineralogy and geochemistry with water chemistry and available monitoring results, it becomes evident that redox cycling of manganese in

conjunction with precipitation of authigenic carbonates largely controls the mobility of dissolved Zn from Christal Lake to Christal Creek at the Silver Trail Highway, where the current study is focussed. The primary source of manganese in the Keno Hill area is weathering of manganese-rich siderite associated with the silver mineralization. Owing to their large specific surface areas, secondary manganese oxides are potent sorbents of heavy metals including zinc. However, as manganese oxides occupy a relatively high position in the redox ladder (Borch et al., 2010), authigenic manganese oxides are susceptible to re-dissolution when the environs turn suboxic, releasing the sorbed metals in the process. In the study area, seasonal changes in dissolved manganese concentrations in the drainage system under an ice cover during the winter months (November to April) is reflective of manganese-oxide dissolution. On the other hand, the released zinc, does not travel far because of its immediate sequestration by precipitating carbonates. As the ice cover starts to melt as the temperature rises (May to October) and as dilution becomes significant due to the melting ice and inflow of new fresh water, some of the carbonates may be re-dissolved. However, the drainage system then would become oxic and manganese oxides would re-precipitate, limiting the amount of zinc that could remain in solution. The net effect of this cycling process is that it renders the study area a sink for zinc, rather than a source. Given the abundance of manganese in the surrounding areas and the high alkalinity in the drainage system, such a natural zinc attenuation process is expected to last for a long time. The process would end if the drainage system becomes permanently suboxic or acidic.

Implications for Mine Reclamation in the Keno Hill Area

Given the apparent effectiveness of natural processes in attenuating the aqueous transport of zinc and other metals/metalloids in the Christal Lake/Creek drainage system, it is tempting to consider natural attenuation as an option for reclaiming various mines in the Keno Hill mining district. Though cost-effective, further work on three aspects of the natural attenuation process need to be conducted to validate it as a viable option for mine reclamation. First, the current study investigated only a limited stretch of the Christal Creek drainage system (Christal Lake to monitoring stations near the Silver Trail

Highway (2). Records at the last monitoring station upstream of the confluence with the South McQuesten River indicate a slightly higher zinc concentration than those measured at stations by the Highway. The cause of the increase is not known. If different natural processes are occurring in the wetland area between the Highway and the River, they should be identified and adaptive measures developed to assure the performance of natural attenuation. Second, the dissolution and precipitation of manganese oxides/hydroxides and other related phases are known to be microbially mediated (Nealson et al., 1988; Tebo et al., 2004; Borch et al., 2010). To date, no detailed microbial studies from the perspective of metal attenuation have been conducted in the Keno Hill area. The subject remains a knowledge gap, which should be addressed to advance natural attenuation as an aid to mine reclamation in the area. Third, the Keno Hill mining district is located in a cold climate region with discontinuous permafrost; natural metal attenuation processes would differ significantly from those occurring in southern climates. For example, the mineralogical studies presented above indicate a slowly evolving but dynamic system in which new minerals are continually forming with aging and cryogenic mineral precipitation as described by Kwong (1997) is a common occurrence in drainage systems across the mining district. In view of a global warming trend, the impact of a changing climate on the prevailing metal attenuation processes must be comprehensively investigated before the longevity of natural attenuation can be ascertained.

CONCLUSIONS

In summary, the current work integrates sediment age-dating, geochemistry and mineralogy with water chemistry and monitoring records to determine the metal background and mobility along the Christal Lake/Creek drainage system. Major conclusions that can be drawn from the various analyses are listed below. Assuming that similar mineralization and natural metal attenuation processes occur across the region, these conclusions are applicable to help inform designing proper strategies for reclaiming

old mine sites, and mine waste management for new operating or developing mines in the entire Keno Hill mining district.

1. Sediments and hence soils in mineralized terrains in the district are enriched in As, Cd, Zn and, to a lesser extent, Cu, Ni and Pb. Given the naturally elevated metal/metalloid levels, site/drainage-specific sediment quality guidelines should be considered for on-going mine reclamation and new operations.

2. While Zn and presumably Cd are readily mobilized in drainage systems, As, Cu, Ni and Pb are not. Sorption and sequestration of Zn with Mn-oxides and authigenic carbonates render Christal Lake a net sink for Zn overall.

3. Seasonal changes in dissolved Zn and Mn concentration in Christal Lake and along Christal Creek demonstrate the significance of Mn-oxide cycling and cryogenic carbonate precipitation in controlling metal remobilization in the drainage system. Such processes will last so long as the environment does not change; for example the drainage system somehow turns acidic or becomes permanently suboxic.

4. To determine if natural attenuation is likely to provide a long-term benefit to reduce metal contaminant loads from various historic mines in the district, further work is required to clarify the role of microbes in effecting metal solubilisation and precipitation in the pertinent drainage systems. In addition, the current study investigated only Christal Lake and the upper reach of Christal Creek. Detailed processes occurring in the wetland area downstream, partially underlain by permafrost, should be identified to validate the applicability of natural attenuation to mitigate metal contamination even in a changing climate.

As a final remark, it should be noted that the present study considers primarily the geochemical processes likely interacting at the study site. There has not been an attempt to conduct a mass-balance accounting between seasonal capture and release of Zn in this

system nor a consideration of possible critical life stages of biota in the Christal Creek system in relation to Zn levels. Such follow-up studies are desirable to fully understand natural metal attenuation in the drainage system.

ACKNOWLEDGEMENTS

We thank Dr. Gary Stern of Fisheries and Oceans Canada for co-ordinating the ^{210}Pb dating of the Christal Lake sediment core at the Fresh Water Institute, Winnipeg, and the associated geochemical analysis at ACME Laboratories Ltd. in Vancouver. The efforts of Environment Canada's analytical laboratory, the Pacific Environment Science Centre in North Vancouver and the Analytical Service Group of CanmetMINING, Ottawa, in providing timely analyses of other water and sediments samples are much appreciated. Derek Smith and Micheline Boisclair of CanmetMINING kindly assisted in sample analysis by XRD and XRF, respectively. The sharing of monitoring data by the Access Consulting Group, Whitehorse, facilitated a much more comprehensive understanding of metal mobilization in the study area than otherwise possible. Lastly, this report has benefited from the peer review by Dr. Suzanne Beauchemin, Charlene Hogan and Bryan Tisch of CanmetMINING from both a technical and management perspective.

REFERENCES

Appelby, P.G. and Oldfield, F. (1978): The calculation of ^{210}Pb dates assuming a constant rate of supply of unsupported ^{210}Pb to the sediments. *Catina* **5**:1-8.

Borch, T., Kretzschmar, R., Kappler, A., van Cappellen, P., Ginder-Vogel, M., Voegelin, A., and Campbell, K. (2010): Biogeochemical redox processes and their impact on contaminant dynamics. *Environmental Sciences and Technology* **44**:15-23.

Boyle, R.W. (1965): Geology, geochemistry and origin of the lead-zinc silver deposits of the Keno-galena Hill area, Yukon Territory. Geological Survey of Canada, Bulletin 111.

Hageman, P.L. (2005): A simple field leach test to assess potential leaching of soluble constituents from mine wastes, soils, and other geologic materials: U.S. Geological Survey Fact Sheet 2005-3100, 4p.

Hageman, P.L. (2007): U.S. Geological Survey field leach test for assessing water reactivity and leaching potential of mine wastes, soils, and other geologic and environmental materials: U.S. Geological Survey Techniques and Methods, book 5, chap. D3, 14p.

Interralogic Inc. (2012): Natural attenuation evaluation, United Keno Hill Mines, Elsa, Yukon. Draft report prepared for the Elsa Reclamation Development Company, Ltd., March 2012, 337pp.

Kwong, Y.T.J., Roots, C.F., Roach, P. and Kettley, W. (1997): Post-mine metal transport and attenuation in the Keno Hill mining district, central Yukon, Canada. *Environmental Geology* **30**:98-107.

Levinson, A.A. (1980): Introduction to Exploration Geochemistry, Second Edition, Applied Publishing Ltd, Wilmette, Illinois, 924pp.

Nealson, K.H., Tebo, B.M. and Rosson, R.A. (1988): Occurrence and mechanisms of microbial oxidation of manganese. *Adv. Appl. Microbiol.* **33**:279-318.

Tebo, B.M., Bargar, J.R., Clement, B.G., Dick, G.J., Murray, K.J., Parker, D., Verity, R. and Webb, S.M. (2004) Biogenic manganese oxides: Properties and mechanisms of formation. *Ann. Rev. Earth Planet. Sci* **32**:287-328.

Wilkinson, P. and Simpson, S.L. (2003): Radiochemical analysis of Lake Winnipeg 99-900 cores 4 and 8. Natural Resources Canada, Geological Survey of Canada: Open File 4196, pp.91-119.

Appendix 1. XRF analyses of selected metals in cored sediments from Christal Lake and Creek

Sample name		Fe	Mn	Pb	Ti	Zn
Core	interval	± 0.04%	± 0.02%	± 0.01%	± 0.04%	± 0.01%
G1-1	0-9 cm	4.54	0.01	<0.01	<0.04	0.10
G1-2	9-18 cm	4.18	0.04	<0.01	0.25	0.15
G1-3	18-27 cm	4.26	0.01	<0.01	0.27	0.11
G1-4	27-36	4.24	0.04	<0.01	0.25	0.11
G2-1	0-9 cm	4.28	0.09	<0.01	<0.04	0.24
G2-2	9-18 cm	4.30	0.06	<0.01	<0.04	0.25
G2-3	18-24 cm	4.28	0.04	<0.01	0.19	0.13
C-1	0-4 cm	2.56	1.09	<0.01	0.23	0.66
C-2	4-8 cm	2.46	1.42	<0.01	<0.04	0.67
C-3	8-12 cm	2.71	1.78	<0.01	<0.04	0.66
C-4	12-16 cm	2.47	1.61	<0.01	<0.04	0.50
C-5	16-20 cm	3.04	1.09	<0.01	<0.04	0.45
C-6	20-24 cm	3.78	0.30	<0.01	0.31	0.21
C-7	24-28 cm	3.91	0.15	<0.01	0.34	0.20
C-8	28-32 cm	4.13	0.07	<0.01	0.31	0.12
C-9	32-36 cm	5.63	0.04	<0.01	0.25	0.06
C-10	36-40 cm	4.24	0.04	<0.01	0.27	0.09
B1-1	0-10 cm	8.12	4.10	<0.01	0.33	1.47
B1-2	~10-20cm	4.16	0.09	<0.01	0.25	0.13
B1-3	~20-30cm	4.09	0.05	<0.01	0.43	0.06
B1-4	~30-40.5	4.12	0.05	<0.01	0.41	0.05
A-1	0-9 cm	4.13	0.04	<0.01	0.35	0.08
A-2	9-18 cm	6.62	0.05	<0.01	0.26	0.05
A-3	18-27 cm	4.81	0.04	<0.01	0.25	0.04
A-4	27-36 cm	4.17	0.03	<0.01	0.38	0.05
CL1-1	0-3 cm	3.22	0.47	<0.01	0.31	0.56
CL1-2	3-15 cm	3.39	0.47	<0.01	0.32	0.41
CL1-3	15-26.5	3.75	0.21	<0.01	0.43	0.21
CL2-1	0-4 cm	2.89	0.08	<0.01	0.27	0.09
CL2-2	4-13 cm	3.30	0.07	<0.01	0.25	0.08
CL2-3	13-22 cm	3.10	0.06	<0.01	0.28	0.10
CCR1-1	0-9 cm	5.65	8.98	0.07	0.39	1.97
CCR1-2	9-18 cm	4.95	9.00	0.11	0.34	1.64
CCR1-3	18-27 cm	4.76	19.94	0.13	<0.04	3.41
CCR1-4	27-36 cm	5.73	1.08	<0.01	0.31	1.51
CCR2-1	0-9 cm	2.95	1.00	0.31	0.32	2.46
CCR2-2	9-18 cm	3.49	0.23	0.08	0.53	0.26
CCR2-3	18-27 cm	2.99	0.37	0.27	0.39	0.48
CCR2-4	27-40 cm	8.73	3.00	0.76	<0.04	5.05
CCR3-1	0-10 cm	3.36	0.45	0.11	0.32	0.33
CCR3-2	10-20 cm	4.02	0.85	0.28	0.29	1.18
CCR3-3	20-30 cm	3.82	0.87	0.33	0.26	1.43
DSKR1-1	0-12 cm	5.12	5.52	0.48	0.30	0.94
DSKR1-2	12-31 cm	2.97	0.01	0.04	0.33	0.05
DSKR2-1	0-3cm	3.76	1.97	0.37	0.30	0.47
DSKR2-2	3-10 cm	2.99	0.87	0.14	0.38	0.21
DSKR2-3	10-15 cm	4.09	2.07	0.37	0.36	0.50

Note: 1) See Figure 2 in the main text for site locations; 2) trace Ni (0.07%) was also detected in sample CCR1-3.

Appendix 2. Selected results of the distilled-water leach test on sediments.

Sample	Depth	Al	As	Ca	Cd	Co	Cu	Fe	K	Mg
	cm	<------	------	------	------	- mg/L -	------	------	------	---->
DSKR1-1	0-12	<0.25	<0.64	161	<0.037	<0.057	<0.016	0.087	1.03	20.9
DSKR1-1dup		<0.25	<0.64	161	<0.037	<0.057	<0.016	0.076	1.06	20.8
DSKR1-2	12-31	<0.25	<0.64	141	<0.037	<0.057	<0.016	0.872	1.67	20.9
DSKR2-1	0-3	<0.25	<0.64	198	<0.037	<0.057	<0.016	0.092	1.19	28.7
DSKR2-2	3-10	<0.25	<0.64	125	<0.037	<0.057	<0.016	0.148	1.24	18.6
DSKR2-3	10-15	<0.25	<0.64	165	<0.037	<0.057	<0.016	0.098	1.02	25.7
CCR3-1	1-10	<0.25	<0.64	123	<0.037	<0.057	<0.016	0.270	1.19	18.4
CCR3-2	10-20	<0.25	<0.64	149	<0.037	0.117	<0.016	0.188	1.64	31.0
CCR3-3	20-30	<0.25	<0.64	263	0.092	0.334	0.023	0.884	1.79	71.0
CCR2-1	0-9	<0.25	<0.64	149	0.056	<0.057	0.018	0.28	1.38	34.6
CCR2-2	9-20	<0.25	<0.64	247	<0.037	<0.057	<0.016	10.2	1.64	34.5
CCR2-3	20-27	<0.25	<0.64	141	<0.037	<0.057	<0.016	1.44	1.55	20.0
CCR2-4	27-40	<0.25	<0.64	61.9	1.94	0.147	<0.016	0.097	1.27	7.75
CCR1-1	0-9	<0.25	<0.64	301	<0.037	<0.057	0.019	0.083	1.87	38.7
CCR1-2	9-18	<0.25	<0.64	274	<0.037	<0.057	<0.016	0.468	1.51	34.9
CCR1-3	18-27	<0.25	<0.64	255	<0.037	<0.057	<0.016	0.054	0.97	24.2
CCR1-4	27-36	<0.25	<0.64	358	0.484	<0.057	<0.016	0.240	2.64	37.6
CL1-1	0-3	<0.25	<0.64	440	<0.037	<0.057	<0.016	5.81	3.46	33.0
CL1-2	3-15	<0.25	<0.64	384	<0.037	<0.057	<0.016	0.260	3.54	31.7
CL1-3	15-26.5	<0.25	<0.64	205	<0.037	<0.057	<0.016	0.222	2.07	33.7
CL2-1	0-4	<0.25	<0.64	201	<0.037	<0.057	<0.016	0.384	1.94	16.5
CL2-2	4-13	<0.25	<0.64	142	<0.037	<0.057	<0.016	0.132	2.21	10.4
CL2-3	13-22	<0.25	<0.64	84.1	<0.037	<0.057	0.038	0.119	1.66	5.16
CL2-3 dup		<0.25	<0.64	83.9	<0.037	<0.057	0.036	0.112	1.90	5.12
Blank		<0.25	<0.64	<0.15	<0.037	<0.057	<0.016	<0.040	<0.58	<0.049
CL-B-1	0-10	<0.25	<0.64	552	0.069	<0.057	<0.016	0.182	1.81	66.2
CL-B-1 dup		<0.25	<0.64	545	<0.037	<0.057	<0.016	2.18	1.97	66.9
CL-B-2	10-20	20.3	<0.41	439	0.104	<0.029	0.017	327	2.48	72.1
CL-B-3	20-30	<0.20	<0.41	354	<0.029	<0.029	0.029	183	2.07	60.6
CL-B-4	30-40.5	<0.20	<0.41	353	0.058	<0.029	0.013	131	1.59	90.7
CL-C-1	1-4	<0.25	<0.64	443	<0.037	<0.057	<0.016	0.251	1.52	23.7
CL-C-2	4-8	<0.25	<0.64	404	<0.037	<0.057	<0.016	0.096	2.04	20.6
CL-C-3	8-12	<0.25	<0.64	361	<0.037	<0.057	<0.016	1.28	1.85	19.1
CL-C-4	12-16	<0.25	<0.64	341	<0.037	<0.057	<0.016	0.256	0.93	19.8
CL-C-4 dup		<0.25	<0.64	338	<0.037	<0.057	<0.016	0.257	0.80	19.9
CL-C-5	16-20	<0.25	<0.64	327	<0.037	<0.057	<0.016	0.080	0.77	21.4
CL-C-6	20-24	<0.25	<0.64	385	<0.037	0.091	<0.016	2.23	0.87	35.2
CL-C-7	24-28	32.5	1.40	371	0.072	0.26	0.016	55.9	4.84	76.7
CL-C-8	28-32	92.2	1.42	339	<0.029	0.29	0.02	103	5.82	98.7
CL-C-9	32-36	51.3	0.98	374	0.147	0.12	0.016	636	3.92	95.3
CL-C-10	36-40	0.31	<0.041	367	<0.029	<0.029	<0.011	234	1.83	52.9
CL-G1-1	1-9	450	6.60	454	0.648	2.06	2.88	2000	<0.58	114
CL-G1-1dup		505	11.8	136	0.763	2.23	3.02	2100	<0.58	126
CL-G1-2	9-18	41.6	2.81	505	0.070	0.127	0.029	114	5.12	89.4
CL-G1-3	18-27	90.4	3.70	394	0.063	0.287	0.017	88.4	7.29	110
CL-G1-4	27-36	<0.20	<0.41	421	<0.029	0.078	0.021	35.4	6.89	108
CL-G2-1	0-9	89.0	1.85	397	0.059	0.519	0.032	150	6.08	79.9
CL-G2-2	9-18	12.5	1.40	512	<0.037	0.369	0.022	40.6	9.74	75.3
CL-G2-3	18.24	169	4.67	423	<0.029	0.408	0.031	188	8.73	128

Appendix 2 (continued). Selected results of the distilled-water leach test on sediments.

Sample	Depth	Mn	Na	Ni	P	Pb	S	Si	Sr	Zn
	cm	<----	------	-----	------	- mg/L -	------	------	------	---->
DSKR1-1	0-12	0.15	3.01	<0.15	<0.31	<0.26	148	2.65	0.284	0.42
DSKR1-1dup		0.15	3.01	<0.15	<0.31	<0.26	149	2.58	0.282	0.43
DSKR1-2	12-31	3.88	3.98	<0.15	<0.31	<0.26	137	3.23	0.224	0.28
DSKR2-1	0-3	0.14	3.38	<0.15	<0.31	<0.26	186	4.81	0.332	1.08
DSKR2-2	3-10	2.07	3.21	<0.15	<0.31	<0.26	122	2.45	0.218	2.23
DSKR2-3	10-15	0.47	3.40	<0.15	<0.31	<0.26	166	3.05	0.285	7.40
CCR3-1	1-10	3.76	3.10	<0.15	<0.31	<0.26	116	3.15	0.200	1.11
CCR3-2	10-20	182	3.10	0.20	<0.31	<0.26	275	4.02	0.293	35.3
CCR3-3	20-30	474	2.93	0.68	<0.31	0.44	638	5.52	0.548	142
CCR2-1	0-9	162	4.01	<0.15	0.60	0.60	262	3.26	0.404	28.7
CCR2-2	9-20	115	4.13	<0.15	<0.31	1.19	307	4.42	0.639	0.47
CCR2-3	20-27	78.1	4.18	<0.15	<0.31	0.49	177	3.00	0.400	1.32
CCR2-4	27-40	213	3.89	0.26	<0.31	1.12	278	1.10	0.011	223
CCR1-1	0-9	20.0	3.71	0.20	<0.31	<0.26	288	10.4	0.411	2.96
CCR1-2	9-18	3.34	4.06	<0.15	<0.31	<0.26	247	8.52	0.357	0.89
CCR1-3	18-27	0.24	2.98	<0.15	<0.31	<0.26	207	10.6	0.402	0.42
CCR1-4	27-36	126	4.23	0.29	<0.31	<0.26	415	2.37	0.323	44.0
CL1-1	0-3	6.52	3.96	<0.15	<0.31	0.35	387	4.90	0.574	4.38
CL1-2	3-15	14.3	3.31	<0.15	<0.31	<0.26	342	3.26	0.522	0.40
CL1-3	15-26.5	8.35	3.21	<0.15	<0.31	<0.26	206	1.40	0.331	<0.14
CL2-1	0-4	0.27	2.16	<0.15	<0.31	<0.26	172	4.00	0.284	<0.14
CL2-2	4-13	0.15	2.71	<0.15	<0.31	<0.26	116	0.88	0.247	<0.14
CL2-3	13-22	0.20	2.85	<0.15	<0.31	<0.26	63.0	0.87	0.161	<0.14
CL2-3 dup		0.20	2.79	<0.15	<0.31	<0.26	63.6	0.88	0.16	<0.14
Blank		<0.012	<0.21	<0.15	<0.31	<0.26	<1.92	<0.10	<0.0042	<0.14
CL-B-1	0-10	278	5.97	0.49	<0.31	<0.26	682	16.4	0.686	15.2
CL-B-1 dup		289	6.26	0.52	<0.31	<0.26	684	14.3	0.666	12.0
CL-B-2	10-20	135	4.76	0.32	0.57	7.85	795	18.7	0.538	16.8
CL-B-3	20-30	32.3	4.24	<0.21	<0.38	<0.38	504	7.11	0.385	0.31
CL-B-4	30-40.5	51.0	4.02	<0.21	<0.38	0.97	528	6.90	0.472	5.18
CL-C-1	1-4	2.71	3.36	<0.15	<0.31	<0.26	347	6.18	0.409	2.55
CL-C-2	4-8	0.34	3.76	<0.15	<0.31	<0.26	326	5.85	0.337	0.87
CL-C-3	8-12	2.93	4.25	<0.15	<0.31	<0.26	297	4.83	0.307	<0.14
CL-C-4	12-16	5.11	3.83	<0.15	<0.31	<0.26	281	4.61	0.325	0.21
CL-C-4 dup		5.09	3.77	<0.15	<0.31	<0.26	280	4.61	0.324	0.20
CL-C-5	16-20	7.05	3.36	<0.15	<0.31	<0.26	278	5.07	0.356	0.31
CL-C-6	20-24	220	3.14	0.18	<0.31	<0.26	470	7.61	0.545	3.27
CL-C-7	24-28	258	5.04	5.59	0.61	1.13	686	20.8	1.08	28.6
CL-C-8	28-32	112	4.43	0.75	<0.38	0.82	759	21.7	1.48	42.3
CL-C-9	32-36	52.6	4.02	1.17	<0.38	0.57	973	16.8	1.59	25.0
CL-C-10	36-40	50.2	3.85	0.25	<0.38	<0.38	554	12.1	1.07	5.62
CL-G1-1	1-9	56.3	4.02	2.94	3.38	0.53	3060	20.8	0.697	165
CL-G1-1dup		63.5	2.16	3.23	5.88	0.67	2990	21.7	0.564	185
CL-G1-2	9-18	41.6	3.11	0.42	0.69	<0.38	741	22.3	1.00	25.7
CL-G1-3	18-27	44.5	3.92	0.59	<0.31	<0.26	723	23.4	1.15	30.9
CL-G1-4	27-36	32.9	4.83	<0.21	<0.38	<0.38	545	3.49	1.05	0.39
CL-G2-1	0-9	110	3.54	1.59	<0.38	<0.38	887	23.0	1.01	150
CL-G2-2	9-18	55.3	4.35	0.74	<0.31	<0.26	603	19.5	1.10	44.6
CL-G2-3	18.24	52.7	4.08	1.10	<0.38	<0.38	1050	23.6	1.27	64.3